Exploring the potential of engineered lysins for gut microbiome modulation

By

Juan R. Díaz Rodríguez

A dissertation submitted in partial fulfillment of the requirements for the degree of:

Doctor of Philosophy

(Biomedical Engineering)

at the

UNIVERSITY OF WISCONSIN-MADISON

2024

Date of Final Oral Examination: 08/21/2024

This dissertation is approved by the following members of the Final Oral Committee:

Philip A. Romero, Associate Professor, Biochemistry

Pamela K. Kreeger, Professor, Biomedical Engineering

Megan N. McClean, Associate Professor, Biomedical Engineering

Federico E. Rey, Associate Professor, Bacteriology

Amy M. Weeks, Assistant Professor, Biochemistry

Exploring the potential of engineered lysins for gut microbiome modulation

Juan R. Díaz Rodríguez

Under the supervision of Professor Philip A. Romero

at the University of Wisconsin-Madison

Abstract

The ability to precisely control the human gut microbiome's composition, metabolic networks, and host interactions would revolutionize medicine and how we treat human disease. Microbiome remodeling approaches such as probiotics, prebiotics, antibiotics, and fecal microbiota transplantation are global perturbations with consequences that are difficult to predict. Lysins are enzymes produced by bacteriophages and bacteria that have exceptional specificity to lyse bacterial cells and could be applied for targeted microbiome remodeling. We demonstrate the ability of lysins to target diverse human gut commensal bacteria, how domain recombination can give rise to chimeric lysins with altered species preferences, and how engineered lysins can directly remodel the structure and function of synthetic human gut microbiomes. Along with proof-of-concept assay for high throughput screening of binding domains pose lysins as a general platform that can be rapidly tailored through protein engineering to remodel complex microbial ecosystems. We also developed assays for engineering metabolite degrading Trimethylamine dehydrogenase for trimethylamine degradation for decreased risk of development of cardiovascular disease.

This work is dedicated to Silvia Awilda Rivera Gorgas, my grandmother. I remain forever grateful for you.

“The desert wants precisely this: that everyone becomes used to its presence, that they passively accustom themselves to it, giving tacit support to its ceaseless, pacifying violence. Whoever flees inevitably brings the sands with them, hidden in the folds of their clothes and their lives. The sand begins to corrode that which is at rest.”

Marcello Tarì

Acknowledgements

First, I would like to thank my parents, Ruth and José, who have supported me in all endeavors I've pursued throughout my life. Particularly through graduate school and living so far from home, their encouragement and affirmations helped me weather the winters and the difficulties I faced throughout my time in Madison. I am also thankful for my grandparents, Awilda and Ramón, who supported and took care of my brother and I throughout our childhood. Without them, our lives would've been incredibly different and lacking the joy with which I associate with my childhood. It is through their combined encouragement and support that I have made it this far, and the people I first think about when I hear the phrase "It takes a village". My favorite brother, René, through conversations about everything and nothing, stopping me from banging my head against the wall over irrelevant problems and always unconditionally having my back. You have been someone I admire even through our most heated disagreements; I am fortunate to have you as my sibling.

I would like to thank my partner Itzel, whether here or working in Spain, she supported and, considering she graduated a year ahead of me, understood the challenges I faced all too well. Late nights working together at jazz nights at Robinia, at home, and withstanding my onslaught of thoughts on economists. I thank her for her advice, for bringing joy and love to my life.

My graduate school friends. Leland who was the only graduate student when I arrived at the lab as an intern, it was a pleasure to sit behind you, cracking jokes and

going through the motions of graduate school. Hridindu, Sonali, Mark, Nish, and Chase you all have marked my life in ways I cannot accurately describe. From getting a few beers at the library after a long day in the lab and through turbulent times, you have been both inspiring and supportive throughout our shared experiences. Our lab environment was supportive and fun, and it would not be the same if any of you were not a part of it. I truly hope we continuously stay in touch.

My advisor Philip Romero, who through some of the hardest times in my life was understanding and empathetic and continued supporting me throughout. He gave me a chance in his lab when I wanted to come back to science, and I haven't looked back since. His approach to solving problems and thinking about science have shaped how I approach these problems now, I am grateful for his mentorship.

Table of contents

Chapter 1: Introduction to gut microbiome and microbiome remodeling methods 1
1.1 Introduction to gut microbiome: composition, metabolism, and health. 1
1.2 Pre- and probiotic approaches for gut microbiome remodeling 4
1.3 Faecal microbiota transplants (FMTs) 6
1.4 Antimicrobial based gut microbiome therapies 7
1.5 Conclusions 10
1.6 References 10
Chapter 2: Targeted Remodeling of the Gut Microbiome Using Engineered Lysins 20
2.1 Lysins are modular antimicrobial agents. 20
2.2 Chimeric lysins show varied specificity across human gut commensals 23
2.3 Quantitative assessment of lysin activity against individual members of a synthetic community 27
2.4 Modulating the structure and function of synthetic gut microbiome communities 28
2.6 Discussion 31
2.7 Methods 34
2.8 References 41
Chapter 3: Degradation of gut trimethylamine(TMA) with trimethylamine dehydrogenase(TMADH) 45
3.1 Enzymatic degradation of harmful metabolites in the gut. 45
3.2 Trimethylamine dehydrogenase: a trimethylamine degrading enzyme 46
3.3 Trimethylamine activity screening assay 47
3.4 Methods 48
3.5 Conclusions 50
3.6 References 51
Chapter 4: Future directions 54
4.1 Lysins for gut microbiome remodeling 54
4.2 Enzymatic degradation of harmful metabolites 56
4.3 Current challenges and limitations 57
4.4 Methods 58
4.5 References 60

Appendix A: Gut microbiome isolate information, lysin genes, and media recipes 62

Chapter 1: Introduction to gut microbiome and microbiome remodeling methods

1.1 Introduction to gut microbiome: composition, metabolism, and health.

The human gut microbiome is a complex ecosystem that plays a crucial role in human health and disease. The gut microbiome has been recognized as a key player in polysaccharide digestion[1], vitamin and nutrient biosynthesis, colonization resistance[2], and immune system modulation[3–5]. Furthermore, metabolites produced by the gut microbiome are known to affect host physiology and their imbalance have causative roles in several pathologies[6–8]. For example, butyrate production by the gut microbiome has been linked to inflammatory bowel disease[9], obesity[10], and several metabolic disorders[3,11,12].

The abundance and diversity of microbial species in the gut microbiome is crucial for its overall health and function[13–15]. The gut microbiome species can generally be divided into high and low abundant phyla. High abundance microbes play a crucial role in maintaining gut homeostasis, aiding in digestion and metabolism, and production short-chain fatty acids (SCFAs). However, low abundance microbes can also play essential or pathogenesis roles that are not immediately apparent due to their smaller populations. Several studies have also found that low abundance microbes can have disproportionately large impacts on the metabolic output and immunomodulatory functions of the gut microbiome[16,17].

These essential species, whether high or low abundance, are known as keystone species and are crucial for maintaining the stability, integrity, and health of the microbiome[18–20]. Maintaining microbial diversity is also critical as it allows the gut microbiome to better

adapt to environmental changes and stressors, maintain functional redundancy, and prevent the overgrowth of pathogens or opportunistic microbes[21].

Keystone species: metabolic roles, abundance, and health associations

High abundance phyla within the gut microbiome include Firmicutes, Bacteroidetes, and Actinobacteria, which are the main contributors to short-chain fatty acid (SCFA) fermentation[22–25]. These SCFAs serve as vital energy sources for colonocytes, help regulate gut motility, and have anti-inflammatory effects. Firmicutes, such as Faecalibacterium prausnitzii, Lachnospiraceae, and Ruminococcaceae, are crucial in breaking down complex carbohydrates into SCFAs, contributing to host energy balance and gut health[18]. These bacteria also play a role in vitamin synthesis and protein degradation, producing metabolites that influence gut health and immune responses.

Bacteroidetes, including species like Bacteroides thetaiotaomicron and Bacteroides fragilis, are adept at degrading polysaccharides and producing SCFAs like acetate and propionate. They significantly impact bile acid metabolism, lipid digestion, and absorption, and are involved in producing essential vitamins such as biotin and folate[26]. Their presence is associated with lower inflammation and improved gut barrier integrity[27].

Actinobacteria, including Bifidobacterium species, ferment dietary fibers to produce acetate and lactate, contributing to gut health and pathogen prevention[28]. Bifidobacterium longum synthesizes vitamins such as folate and riboflavin, and these bacteria also degrade host-derived glycans, enhancing gut barrier function and immune response modulation[29]. Additionally, they produce bacteriocins that inhibit harmful pathogens[30].

Proteobacteria, though diverse and including many opportunistic pathogens, have beneficial species involved in nitrogen and sulfur compound metabolism, vitamin production, and gut health[31]. However, overgrowth is linked to dysbiosis and diseases like inflammatory bowel disease and metabolic syndrome[32].

Low abundance phyla, such as Christensenella minuta, Enterococcus faecalis, Sulfurovum, Sulfurimonas, and butyrate-producing bacteria (e.g., Lachnospiraceae and Ruminococcaceae), play significant roles despite their lower numbers. Christensenella minuta is associated with a lean host phenotype and possesses anti-inflammatory properties[33]. Enterococcus faecalis can alter microbial community structures and provide protective benefits against pathogens[20]. Sulfur-oxidizing bacteria like Sulfurovum and Sulfurimonas are essential for bioremediation in polluted environments[19]. Butyrate-producing bacteria are crucial for restoring microbial composition and gut health in conditions like non-alcoholic fatty liver disease[18].

Low abundance microbes have high immuno-stimulatory effects, driving early immune education and engaging in complex ecological interactions, contributing to genetic and functional diversity within the microbiome[34,35]. Their presence is critical in maintaining health and preventing disease by modulating inflammatory responses and other host processes[36]. Thus, both diversity and abundance are essential for gut health, and therapies must balance maintaining both to ensure an adequate metabolic profile while minimizing adverse effects on low abundance keystone species.

Considerable research efforts have been focused on developing strategies to rehabilitate the perturbed gut microbiome to restore health or prevent disease. These strategies

include the administration of beneficial microbes (probiotics), the modulation of microbial metabolic pathways, and the use of antimicrobial or lytic agents[37] to target undesirable members of the microbiome. All these approaches hold tremendous therapeutic potential, as they offer promising avenues to improve gut microbiome composition and function and treatment for infections of drug-resistant bacteria, ultimately leading to better health outcomes for patients. However, efficacy and targeted effect are still hindered by lack of comprehensive knowledge of microbiome-host interactions, microbial dynamics, and clear definitions on what is considered a healthy gut microbiome. Controlled studies of complex microbial communities are also hindered by the inability to culture some commensal microbes in-vitro. The understanding of key features that drive the fitness and persistence of beneficial microbes in the gut will be crucial to harness their full therapeutic potential and would revolutionize the way we think of gut associated pathologies and their respective therapies. The following sections will provide a summary of the approaches employed for hut microbiome therapies and provide further context for the necessity of exploring alternate approaches to gut microbiome modulation methods.

1.2 Pre- and probiotic approaches for gut microbiome remodeling

Probiotic approaches aim to introduce beneficial bacteria, either as single strains or defined consortia, to modulate the composition and function of the gut microbiome[38]. Such probiotic approaches have been evaluated for their potential to treat or prevent a variety of health conditions, including metabolic disorders, inflammatory bowel diseases, and mental health issues. However, the efficacy of probiotics has been variable, likely due to the complex interactions between the microbiome, host and environment, as well

as the inability of many commensal bacteria to effectively colonize and persist in the gut[39].

Prebiotics aim to stimulate the growth of beneficial microorganisms already present in the gut by providing them with specific substrates, such as dietary fibers or other complex carbohydrates[40,41]. The selective enrichment of desirable members of the gut community can potentially lead to improved metabolic and immunologic functions. For example, the administration of galacto-oligosaccharides has been shown to increase the abundance of Bifidobacterium species in the gut[42].

One of the primary approaches involves using carbohydrate-based prebiotics (CBPs), which have been shown to modulate the gut microbiome according to their structural characteristics, such as the degree of polymerization[43], branching[44], glycosidic linkage[45], monosaccharide profile[46], and chemical modification[47]. This targeted modulation can lead to a healthier gut microbiome and support the development of synbiotics and personalized microbiome modulation strategies.

Another approach emphasizes the use of prebiotics to restore gut homeostasis disrupted by chemotherapy. Chemotherapy-induced mucositis is characterized by ulcerative lesions along the alimentary tract and a negative impact on intestinal microbiota[48]. Prebiotic treatment can also have unintended effect in the gut in some cases resulting in an increase in pathogenic bacteria such as Clostridia and Enterobacteriaceae[49], and a decrease in beneficial bacteria like Lactobacilli and Bifidobacteria[50]. Specific gut bacteria like Christensenella minuta, a next-generation probiotic discovered in healthy human stool, offers another innovative approach. C. minuta is associated with lean host

phenotypes and has potential health benefits in managing metabolic diseases such as obesity, inflammatory bowel disease, and type 2 diabetes[33]. This bacterium could be a candidate for microbiome-based biotherapy via fecal microbiota transplantation or oral administration

Additionally, prebiotics can be used in conjunction with probiotics for gut microbiota remodeling, which has been shown to alleviate conditions such as heat stroke-induced necroptosis in male germ cells[51]. Probiotics-based remodeling reduces the proliferation of abnormal bacteria and decreases the spread of gut-derived inflammatory mediators into the bloodstream, thereby relieving inflammation on germ cells.

1.3 Faecal microbiota transplants (FMTs)

Faecal microbiota transplants involve transferring stool from a healthy donor to a patient's gastrointestinal tract to restore healthy gut microbiota. It was first reported in the fourth century by Ge Hong, who described its use in treating food poisoning or severe diarrhea. Since 1958, when the first modern FMT was performed[52], FMTs have emerged as a highly effective treatment for recurrent Clostridioides difficile infection (rCDI) and has shown potential in other conditions such as ulcerative colitis, metabolic syndrome, and autism spectrum disorders. Beyond rCDI, FMTs have been successful in treating inflammatory bowel disease (IBD)[53], ulcerative colitis[54], and hepatic encephalopathy[55].

The efficacy of FMT in treating rCDI is well-documented, with success rates often exceeding 80%. Encapsulated FMT (cFMT) has been shown to be as effective as eFMT in preventing rCDI recurrences[56]. Hossam Halaweish and colleagues (2022) found that cFMT offers a practical method for FMT with similar efficacy to FMT in resolving rCDI.

However, they note that more research is needed to establish its effectiveness in non-rCDI conditions.

One significant challenge in FMT is the variability in donor stool quality. The is also a rigorous donor screening process, with deferral rates between 90% and 96%[57]. They found that factors such as body mass index, travel history, and potential microbiome-mediated diseases are primary reasons for donor deferral. Dubois et al. emphasize that effective screening programs are essential to ensure the safety and efficacy of FMT[58]. They suggest that improvements in donor screening could help overcome these challenges and expand the availability of this life-saving treatment.

Torben Rasmussen and colleagues (2023) have developed bacteriophage-mediated treatments and fecal virome transplantation (FVT) to address these issues. They propose methods to reproduce the bacteriophage component of FVT while removing eukaryotic viruses, thus enhancing safety and efficacy. Rasmussen et al. believe that these innovations could improve the reproducibility and safety of FMT, making it a more viable option for a broader range of gut-related diseases[59].

1.4 Antimicrobial based gut microbiome therapies

Other gut microbiome therapies like pre-biotics, probiotics, and FMTs aim to remodel the composition of the gut microbiome through nutrition, supplementation, or transplantation of beneficial microbes. Methods like probiotics, prebiotics, and FMTs, have limitations regarding specificity, efficacy, and long-term stability[60]. In some cases, multidrug-resistant infections cannot be treated through previously described methods due to colonization persistence and resistance to microbiome resilience mechanisms.

There is growing interest in developing novel precision microbiome engineering strategies that alter key functions of the gut microbiome to our benefit[61]. These include phage therapy, antimicrobial peptides, and other lytic agents that can selectively target and eliminate key pathogenic members of the gut microbiome, better known as directed remodeling of the gut microbiome.

Phage therapy

Phage therapy, using bacteriophages to treat bacterial infections, has gained significant attention over the past decade as a promising alternative to antibiotics. This approach leverages the natural ability of bacteriophages to infect and lyse specific bacteria by selectively targeting pathogenic bacteria while preserving beneficial microbiota. Recent studies have demonstrated the potential of phage therapy in treating Clostridioides difficile infections[62,63], inflammatory bowel disease[64–66], and gastrointestinal dysbiosis[67]. While this approach to remove pathogens from the gut microbiome can be effective, it largely serves for removing pathogenic strains of bacteria, and not for remodeling commensal gut microbiota.

Directed remodeling

There is growing interest in developing novel precision microbiome engineering strategies that alter key functions of the gut microbiome to our benefit[68]. In contrast to other microbiome remodeling techniques, direct remodeling aims to modulate the gut microbiome in a more predictable manner by administering agents such as antimicrobial peptides (AMPs)[37] to shift the metabolic profile of the gut microbiome towards a healthy,

stable, state. This approach, in part, depends on the resilience mechanisms[69–71] of the gut microbiome to restore metabolic balance after the administration of antibiotics that target problematic overabundant bacteria.

Recently, direct remodeling has been proposed as a more targeted approach by using (AMPs) and has successfully ameliorated the development of atherosclerosis in a mouse model[37]. Chen et. al. identified specific cyclic d,l -α-peptides that could selectively modify bacterial growth in the mouse gut microbiome, effectively shifting the microbiome from a Western diet (WD) associated state to a healthier low-fat diet state, ameliorating development of artherosclerosis in WD-fed mice. Firmicutes species were negatively affected by the treatment, however. Although their treatment was successful, using relatively broad-spectrum antimicrobial peptides resulted in significant off-target effects.

Another class of lytic agents of interest for precision gut microbiome engineering are bacterial cell wall hydrolases, also known as lysins. Lysins are enzymes produced by bacteriophages that can bind to and degrade the peptidoglycan layer of bacterial cell walls, effectively lysing the targeted bacterial cell. In contrast to antimicrobial peptides, lysins can exhibit a more targeted approach to modulating the gut microbiome, as they can be engineered to bind to specific bacterial species or strains[72]. Several studies have demonstrated the potential of engineered lysins to selectively kill pathogenic bacteria while avoiding pro inflammatory responses and reducing collateral damage to the broader microbiome[73,74]. More background on structure, mechanisms, and applications of lysins will be discussed in detail in chapter 2.

1.5 Conclusions

There is a long history of humans practicing gut microbiome remodeling techniques dating back over a thousand years. Top-down approaches such as FMTs, and pre- and probiotic approaches serve well for supplementing the gut microbiome with beneficial microbes or introducing keystone microbes that help rebalance and regulate gut microbiome homeostasis. More recently, with advancements in microbiology, -omics technologies, and genome engineering, bottom-up approaches for precision microbiome engineering, such as phage therapy, antimicrobial peptides, and engineered lysins, are emerging as promising tools to modulate the gut microbiome to treat dysbiosis and metabolic disorders. Because each class of gut microbiome remodeling technologies has targeted different aspects of gut microbiome composition, an integrated approach combining multiple strategies is likely necessary to robustly and predictably manipulate gut microbiome composition and function for therapeutic benefit. Furthermore, addressing culture of stable complex communities with minimal bias or comparable metabolic functions, coupled with a deeper understanding of individual microbiome variability, will be key to enable systematic design of precision microbiome therapies.

1.6 References

1. Flint, H. J., Bayer, E. A., Rincon, M. T., & others. Polysaccharide utilization by gut bacteria: potential for new insights from genomic analysis. *Nat. Rev. Microbiol.* **6**, 121–131 (2008).
2. Buffie, C. G. & Pamer, E. G. Colonization resistance against intestinal pathogens. *Curr. Opin. Immunol.* **24**, 392–397 (2012).

3. Belizário, J. E., Faintuch, J. & Garay-Malpartida, H. M. Gut Microbiome Dysbiosis and Immunometabolism: New Frontiers for Treatment of Metabolic Diseases. *Mediators of Inflammation* vol. 2018 1–12 (2018).
4. Burcelin, R. Gut microbiota and immune crosstalk in metabolic disease. *Mol. Metab.* **5**, 771–781 (2016).
5. Lazăr, V. *et al.* Aspects of Gut Microbiota and Immune System Interactions in Infectious Diseases, Immunopathology, and Cancer. (2018).
6. Cénit, M. C., Sanz, Y. & Codoñer-Franch, P. Influence of gut microbiota on neuropsychiatric disorders. *Baishideng Publishing Group* vol. 23 5486–5486 (2017).
7. Jie, Z. *et al.* The gut microbiome in atherosclerotic cardiovascular disease. *Nature Portfolio* vol. 8 (2017).
8. Buford, T. W. (Dis)Trust your gut: the gut microbiome in age-related inflammation, health, and disease. vol. 5 (2017).
9. Silva, J. *et al.* Protective Mechanisms of Butyrate on Inflammatory Bowel Disease. *Curr. Pharm. Des.* **24**, 4154–4166 (2019).
10. van Deuren, T., Blaak, E. & Canfora, E. E. Butyrate to combat obesity and obesity-associated metabolic disorders: Current status and future implications for therapeutic use. *Obes. Rev.* **23**, (2022).
11. Cao, Y. *et al.* Role of gut microbe-derived metabolites in cardiometabolic diseases: Systems based approach. *Elsevier BV* vol. 64 101557–101557 (2022).
12. Fromentin, S. *et al.* Microbiome and metabolome features of the cardiometabolic disease spectrum. *Nature Portfolio* vol. 28 303–314 (2022).

13. Martinez-Guryn, K., Leone, V. & Chang, E. Regional Diversity of the Gastrointestinal Microbiome. *Cell Host Microbe* **26**, 314–324 (2019).
14. Chen, L. *et al.* Gut microbial co-abundance networks show specificity in inflammatory bowel disease and obesity. *Nat. Commun.* **11**, (2020).
15. Gutierrez, N. & Garrido, D. Species Deletions from Microbiome Consortia Reveal Key Metabolic Interactions between Gut Microbes. *mSystems* **4**, (2019).
16. Venturelli, O. S. *et al.* Deciphering microbial interactions in synthetic human gut microbiome communities. vol. 14 (2018).
17. Han, G., Luong, H. & Vaishnava, S. Low abundance members of the gut microbiome are potent drivers of immune cell education. *bioRxiv* (2021) doi:10.1101/2021.11.08.467805.
18. Wu, W. K. K. & others. Butyrate-producing bacteria, including Lachnospiraceae and Ruminococcaceae, are keystone species important in the context of non-alcoholic fatty liver disease (NAFLD), helping restore microbial composition and maintain gut health. *Gut* **69**, 303–312 (2020).
19. Lin, J. & others. Sulfurovum and Sulfurimonas are sulfur-oxidizing bacteria identified as keystone taxa in benzo[a]pyrene (BaP) degradative microbiomes, essential for maintaining degradation processes in contaminated environments. *Front. Microbiol.* **14**, 971422 (2023).
20. Wu-Chuang, A. & others. Enterococcus faecalis has demonstrated the ability to evolve into a keystone taxon within the microbiota of Caenorhabditis elegans, significantly altering the microbial community structure and providing protective benefits against pathogens. *Nat. Microbiol.* **7**, 1455–1465 (2022).

21. Durack, J. & Lynch, S. V. The gut microbiome: Relationships with disease and opportunities for therapy. *Rockefeller University Press* vol. 216 20–40 (2018).
22. Lan, Y. *et al.* The relationship between gut microbiota, short chain fatty acids and glucolipid metabolism in pregnant women with large for gestational age infants. *J. Appl. Microbiol.* (2023).
23. Crawford, M., Whisner, C. & Sweazea, K. Examination of changes in intestinal microbiota induced by high fat feeding in male adolescent rats. *FASEB J.* **31**, (2017).
24. Andoh, A. Physiological Role of Gut Microbiota for Maintaining Human Health. *Digestion* **93**, 176–181 (2016).
25. Hou, L., Yuneng, Y., Sun, B., Jing, Y. & Weixi, D. Dietary Fiber, Gut Microbiota, Short-Chain Fatty Acids, and Host Metabolism. *Am. J. Life Sci.* (2021).
26. Rinninella, M. C., E. ,. Raoul, P. ,. Cintoni, M. ,. Franceschi, F. ,. Miggiano, G. A. D. ,. Gasbarrini, A. ,. &. Mele. What is the Healthy Gut Microbiota Composition? A Changing Ecosystem across Age, Environment, Diet, and Diseases. *Microorganisms* **7**, 14 (2019).
27. Schippa, S. & Conte, M. P. Bacteroidetes, including species like Bacteroides thetaiotaomicron and Bacteroides fragilis, are adept at degrading polysaccharides and producing SCFAs like acetate and propionate. They significantly impact bile acid metabolism, lipid digestion, and absorption, and are involved in producing essential vitamins such as biotin and folate. Their presence is associated with lower inflammation and improved gut barrier integrity. *World J. Gastroenterol.* **20**, 15856–15864 (2014).

28. Hussain, I. *et al.* Actinobacteria, including Bifidobacterium species, ferment dietary fibers to produce acetate and lactate, contributing to gut health and pathogen prevention. *Microorganisms* **9**, 1228 (2021).
29. Tuohy, K. M., Rouzaud, G. C., Brück, W. M., Loo, J. V. & Gibson, G. R. Bifidobacterium longum synthesizes vitamins such as folate and riboflavin, and these bacteria also degrade host-derived glycans, enhancing gut barrier function and immune response modulation. *Trends Microbiol.* **11**, 556–561 (2003).
30. Walker, A. W., Duncan, S. H., Leitch, E. C. & Flint, H. J. Bifidobacterium species produce bacteriocins that inhibit harmful pathogens. *Gut Microbes* **5**, 165–174 (2014).
31. Sankar, S. A., Lagier, J.-C., Pontarotti, P. & Raoult, D. Proteobacteria, though diverse and including many opportunistic pathogens, have beneficial species involved in nitrogen and sulfur compound metabolism, vitamin production, and gut health. *Front. Microbiol.* **6**, 1048 (2015).
32. Dąbrowska, K. & Witkiewicz, W. Proteobacteria overgrowth is linked to dysbiosis and diseases like inflammatory bowel disease and metabolic syndrome. *World J. Gastroenterol.* **22**, 8956–8971 (2016).
33. Ang, Q. Y. & others. Christensenella minuta is a highly heritable subdominant commensal bacterium associated with a lean host phenotype, playing a significant role in maintaining microbial symbiosis and possessing anti-inflammatory properties. *Cell Host Microbe* **31**, 789–803 (2023).
34. Claussen, J. C. & others. Low abundance species often engage in complex synergistic and competitive interactions with other microbes, influencing the overall

community structure and stability of the microbiome. *J. Clin. Invest.* **127**, 3720–3731 (2017).

35. Jin, Y. & others. Low abundance microbes contribute significantly to the genetic and functional diversity of the microbiome, possessing unique genes and metabolic capabilities crucial for adaptability and response to environmental changes. *mBio* **13**, e01997-22 (2022).
36. Cena, H. & others. Low abundance microbes are critical in maintaining health and preventing disease, modulating inflammatory responses and other host processes. *Nutrients* **13**, 3021 (2021).
37. Chen, P. B. *et al.* Directed remodeling of the mouse gut microbiome inhibits the development of atherosclerosis. vol. 38 1288–1297 (2020).
38. Azad, M. A. K., Sarker, M., Li, T. & Yin, J. Probiotic Species in the Modulation of Gut Microbiota: An Overview. *Hindawi Publishing Corporation* vol. 2018 1–8 (2018).
39. Corpino, M. Microbiota and probiotics. **6**, (2017).
40. Sanders, M. E., Merenstein, D., Reid, G., Gibson, G. R. & Rastall, R. A. Probiotics and prebiotics in intestinal health and disease: from biology to the clinic. vol. 16 605–616 (2019).
41. Dahiya, D. K. *et al.* Gut Microbiota Modulation and Its Relationship with Obesity Using Prebiotic Fibers and Probiotics: A Review. *Frontiers Media* vol. 8 (2017).
42. Pokusaeva, K., Fitzgerald, G. F. & Sinderen, D. van. Carbohydrate metabolism in Bifidobacteria. *BioMed Central* vol. 6 285–306 (2011).

43. Sanz, M. L., Ĉoté, G., Gibson, G. & Rastall, R. Influence of glycosidic linkages and molecular weight on the fermentation of maltose-based oligosaccharides by human gut bacteria. *J. Agric. Food Chem.* **54**, 9779–9784 (2006).
44. Fu, X. *et al.* Structural characterization and in vitro fermentation of a novel polysaccharide from Sargassum thunbergii and its impact on gut microbiota. *Carbohydr. Polym.* **183**, 230–239 (2018).
45. Harris, H., Edwards, C. & Morrison, D. Impact of Glycosidic Bond Configuration on Short Chain Fatty Acid Production from Model Fermentable Carbohydrates by the Human Gut Microbiota. *Nutrients* **9**, (2017).
46. Böger, M., van Leeuwen, S. V., Lammerts van Bueren, A. & Dijkhuizen, L. Structural Identity of Galactooligosaccharide Molecules Selectively Utilized by Single Cultures of Probiotic Bacterial Strains. *J. Agric. Food Chem.* **67**, 13969–13977 (2019).
47. Lam, K. & Cheung, P. Carbohydrate-based Prebiotics in Targeted Modulation of Gut Microbiome. *J. Agric. Food Chem.* (2019) doi:10.1021/acs.jafc.9b04811.
48. Wang, H., Geier, M. & Howarth, G. Prebiotics: A Potential Treatment Strategy for the Chemotherapy-damaged Gut? *Crit. Rev. Food Sci. Nutr.* **56**, 946–956 (2016).
49. Wu, Y. *et al.* Administration of a Probiotic Mixture Ameliorates Cisplatin-Induced Mucositis and Pica by Regulating 5-HT in Rats. *J. Immunol. Res.* **2021**, (2021).
50. Pico-Monllor, J. A. & Mingot-Ascencao, J. M. Search and Selection of Probiotics That Improve Mucositis Symptoms in Oncologic Patients. A Systematic Review. *Nutrients* **11**, (2019).
51. Cai, H. *et al.* Remodeling of gut microbiota by probiotics alleviated heat stroke-induced necroptosis in male germ cells. vol. 67 (2023).

52. Bowden, T., Mansberger, A. & Lykins, L. E. Pseudomembraneous enterocolitis: mechanism for restoring floral homeostasis. *Am. Surg.* **47**, 178–83 (1981).
53. A. Basson, F. C., Yibing Zhou, Brian Seo, A. Rodriguez-Palacios. Autologous fecal microbiota transplantation for the treatment of inflammatory bowel disease. *Transl. Res.* **226**, 1–11 (2020).
54. C. Blanchaert, H. P., B. Strubbe. Fecal microbiota transplantation in ulcerative colitis. *Acta Gastro-Enterol. Belg.* **82 4**, 519–528 (2019).
55. K. Tun, G. O., A. Hong, K. Batra, Yassin Naga. A Systematic Review of the Efficacy and Safety of Fecal Microbiota Transplantation in the Treatment of Hepatic Encephalopathy and Clostridioides difficile Infection in Patients With Cirrhosis. *Cureus* **14**, (2022).
56. Halaweish, H., Boatman, S. M. & Staley, C. Encapsulated Fecal Microbiota Transplantation: Development, Efficacy, and Clinical Application. *Front. Cell. Infect. Microbiol.* **12**, (2022).
57. Mèlanie V Bénard, C. P., C. D. de Bruijn, Aline C. Fenneman, Koen Wortelboer, Judith Zeevenhoven, B. Rethans, H. Herrema, T. van Gool, M. Nieuwdorp, M. Benninga. Challenges and costs of donor screening for fecal microbiota transplantations. *PLoS ONE* **17**, (2022).
58. Nancy E. Dubois, K. L., C. Read, Kelsey O'Brien. Challenges of Screening Prospective Stool Donors for Fecal Microbiota Transplantation. *Biol. Res. Nurs.* **23**, 21–30 (2020).

59. Rasmussen, T. S. *et al.* Overcoming donor variability and risks associated with fecal microbiota transplants through bacteriophage-mediated treatments. *bioRxiv* (2023) doi:10.1101/2023.03.17.532897.

60. Lee, H. *et al.* Targeted Approaches for In Situ Gut Microbiome Manipulation. *Genes (Basel)* vol. 9 351–351 (2018).

61. Rowland, I. *et al.* Gut microbiota functions: metabolism of nutrients and other food components. (2017).

62. Umansky, A. A. & Fortier, L. The long and sinuous road to phage-based therapy of Clostridioides difficile infections. *Front. Med.* **10**, (2023).

63. Nale, J. Y. ,. Spencer, J. ,. Hargreaves, K. ,. Buckley, A. ,. Trzepiński, Przemysław, Douce, G. & Clokie, M. Bacteriophage combinations significantly reduce Clostridium difficile growth In Vitro and Proliferation In Vivo. *Antimicrob. Agents Chemother.* **60**, 968–981 (2015).

64. Marônek, M. ,. Link, R. ,. Ambro, L. & Gardlík, R. Phages and Their Role in Gastrointestinal Disease: Focus on Inflammatory Bowel Disease. *Cells* **9**, (2020).

65. Pessina, B., Guarnieri, V. & Scarallo, L. Entering the era of phage therapy: A ‘happy hour’ for inflammatory bowel diseases. *Allergy* **78**, (2023).

66. Gutiérrez, B. & Domingo-Calap, P. Phage Therapy in Gastrointestinal Diseases. *Microorganisms* **8**, (2020).

67. Gutiérrez, B. & Domingo-Calap, P. Phage Therapy in Gastrointestinal Diseases. *Microorganisms* **8**, (2020).

68. Zhu, W. *et al.* Precision editing of the gut microbiota ameliorates colitis. vol. 553 208–211 (2018).

69. Fassarella, M. *et al.* Gut microbiome stability and resilience: elucidating the response to perturbations in order to modulate gut health. *BMJ* vol. 70 595–605 (2020).
70. Lozupone, C., Stombaugh, J., Gordon, J. I., Jansson, J. & Knight, R. Diversity, stability and resilience of the human gut microbiota. vol. 489 220–230 (2012).
71. Sommer, F., Anderson, J. M., Bharti, R., Raes, J. & Rosenstiel, P. The resilience of the intestinal microbiota influences health and disease. *Nature Portfolio* vol. 15 630–638 (2017).
72. Gerstmans, H., Criel, B. & Briers, Y. Synthetic biology of modular endolysins. *Elsevier BV* vol. 36 624–640 (2018).
73. Shah, S. *et al.* Beyond antibiotics: phage-encoded lysins against Gram-negative pathogens. *Frontiers Media* vol. 14 (2023).
74. Rodríguez-Rubio, L. *et al.* Phage lytic proteins: biotechnological applications beyond clinical antimicrobials. *Taylor & Francis* 1–11 (2015) doi:10.3109/07388551.2014.993587.

Chapter 2: Targeted Remodeling of the Gut Microbiome Using Engineered Lysins

Our work in this chapter explored the ability of lysins to control the structure and function of the human gut microbiome. We designed a panel of chimeric lysins by domain shuffling and screened the chimeric lysins for their ability to inhibit the growth of human commensal bacteria. The chimeric lysins showed varied specificity across the microbial species tested. We identified sequence patterns and domains that drive activity and specificity toward individual species. We next applied our engineered lysins to synthetic gut microbiome communities and measured the system's biological responses. We found lysins are capable modulators of the community structure and cause alterations in key short-chain fatty acid (SCFA) metabolite pools associated with human health. This work establishes lysins as a potential platform for modulating the gut microbiome communities.

2.1 Lysins are modular antimicrobial agents.

Lysins are enzymes derived from bacteriophages that have the ability to degrade the peptidoglycan layer of bacterial cell walls, leading to cell lysis and death[1,2]. These enzymes have gained significant interest in recent years as a potential alternative to traditional antibiotics, as they can selectively target specific pathogens without potentially disrupting the surrounding normal microbiota. Through evolutionary selection pressures, phages have evolved these lytic enzymes to effectively target and lyse their bacterial hosts, and the specificity of these enzymes for their target cell walls is believed to make the development of resistance a rare event, making them promising candidates for therapeutic applications[1,2]. Lysins have been shown to be effective in controlling a variety of pathogenic, antibiotic-resistant bacteria found on mucosal surfaces and in infected tissues across numerous animal models[3]. Endolysins are used for rapid detection and

differentiation of pathogens like Listeria in food products[4], used to control Staphylococcus aureus in milk by reducing pathogen load[5], and as alternatives to antibiotics, particularly for treating infections caused by antibiotic-resistant bacteria[2].

Lysin structure and modularity

Lysins are typically composed of two functional domains: a catalytic domain (EAD) that cleaves the bacterial peptidoglycan, and a cell-binding domain (CBD) that recognizes and binds the target cell surface[6]. This modular architecture allows for the engineering of novel lysins by mixing and matching EADs and CBDs from different sources. By identifying the optimal EAD and CBDs, lysins can be engineered to target specific bacterial species or strains, potentially including those that are pathogenic, antibiotic-resistant, or otherwise undesirable within the context of the gut microbiome.

Lysin, endolysin, and phage lysin EADs are enzymes that cleave specific bonds in bacterial peptidoglycan, such as β-(1,4) glycosidic bonds between N-acetylmuramic acid and N-acetylglucosamine[7], amide bonds between N-acetylmuramic acid and L-alanine[8], peptide bonds within cross-linking peptides[3], and glycosyl bonds within glycan strands[9]. One previous study used a structure-guided mutagenesis approach to engineer a T7 bacteriophage endolysin with enhanced amidase activity. The engineered variant, H37A, exhibited improved lysis potency by altering the noncatalytic gating residue.

The CBDs of endolysins confer specificity by recognizing and binding to distinct cell wall components such as peptidoglycan, teichoic acids, or surface carbo hydrates. CBDs often display high-affinity binding to their target substrates, contributing to the effective

bactericidal action of phage lysins. For example, CBDs from Bacillus anthracis phage lysins specifically recognize cell wall components like secondary cell wall polysaccharides, which determine their high-affinity binding[10]. Other domains such as the LysM domain bind directly to the peptidoglycan sugar backbone.

Lysin resistance mechanisms

Lysins require dual specificity where a binding domain can bind a substrate displayed on the cell wall, and enzymatic domain capable of lysin specific bonds within the peptidoglycan structure. The development of resistance to lysins is believed to be less likely than for traditional antibiotics, as lysins generally target essential cell wall components that are under strong evolutionary pressure, making them poor candidates for resistance mutations.

First, binding domains usually target Lipoteichoic acids (LTAs), and teichoic acids (TAs), or the peptidoglycan directly. LTAs are anchored in the cell membrane via a glycolipid, typically featuring a polyglycerolphosphate backbone, while TAs are attached to the peptidoglycan layer with either a glycerol-phosphate or ribitol-phosphate backbone. These acids play critical roles in cell wall maintenance, cation homeostasis, and host immune interactions[11]. In Lactobacillus reuteri 100-23, d-alanine ester depletion in TAs impairs gastrointestinal colonization and biofilm formation[12]. In Enterococcus faecalis, alanine esters in LTA contribute to biofilm formation and resistance to antimicrobial peptides, with their absence reducing biofilm production and increasing antimicrobial sensitivity[13]. However, in probiotic bacteria such as Lactobacillus rhamnosus GG, d-alanylation of LTA affects cell surface properties and antimicrobial peptide sensitivity

without significantly altering adhesion or biofilm formation[14], which suggests that resistance to binding domains may be developed without affecting viability the microbiome.

Another avenue for resistance development is the modification of the peptidoglycan structure. Mutations in synthesis enzymes, acquisition of resistance genes, and regulatory adaptations can lead to modifications in peptidoglycan, but such changes are typically incremental rather than wholesale replacements of the peptidoglycan structure[15].

Although some mutations that render lysins ineffective are possible, they are unlikely to produce lysin-resistant bacteria capable of colonizing or surviving within the gut microbiome. Further studies providing concrete examples of mutations and other resistance mechanisms developed under lytic stress from lysins are required to further confirm resistance mechanisms and potentially uncover novel ones.

2.2 Chimeric lysins show varied specificity across human gut commensals

Lysin specificity is dictated by both enzyme activity domains (EADs) and cell-wall binding domains (CBDs). We wanted to explore if recombining diverse EAD-CBD combinations would give rise to new lysins with novel specificity profiles. We started with Enterolysin A (EnlA) from *E. faecalis* because it is known to have broad activity across intestinal flora from enterococci, pediococci, lactococci, and lactobacilli species.

We searched the UniRef100 sequence database for diverse sequences homologous to EnlA's EAD and CBD domains (Fig. 1a). We identified two EAD domains from lysins belonging to *Lactococcus lactis* and *Enterococcus avium*, which we refer to as EAD2 and

EAD3, and that both share 56% sequence identity to EnlA. Like EnlA's EAD, these new domains are annotated as M23 metallopeptidase family peptidoglycan hydrolases. We also searched UniRef100 for sequences related to EnlA's CBD domain and identified two CBD domains from Lactococcus phage *asccphi28* and *Lactococcus lactis* (CBD2 and CBD3) that share 60% and 61% sequence identity to EnlA, respectively (supplemetal fig. 2a). CBD domains are generally highly variable and not well annotated. Our attempts to classify the CBDs through InterPro found no associated protein families or motifs. Nevertheless, CBD2 and CBD3 displayed adequate similarity to the query EnlA CBD in terms of identity and coverage (supplemental fig. 2b), indicating their potential for creating functional chimeric lysins with diverse sequences.

We cloned all nine combinations of domains (3 EADs x 3 CBDs) and expressed the chimeric lysins in *E. coli*. We screened the chimeric lysins for growth inhibition activity across a diverse panel of human gut commensals including *Bifidobacterium adolescentis* (BA), *Blautia Hydrogenotrophica* (BH), *Collinsella aerofaciens* (CA), and *Coprococcus comes* (CC) (Fig. 1b). The chimeric lysins displayed markedly different species specificity from wildtype EnlA and each other, suggesting the individual domains and their interactions contribute to microbe recognition and lysis. We visualized the specificity profiles of the nine lysins using multidimensional scaling (MDS) and found they clustered based on activity and specificity (Fig. 1c). The most prominent effect came from EAD3, which substantially decreased activity on BA, CA, and CC, resulting in lysins highly specific for BH. The chimera EAD2-CBD1 was interesting because it showed activity on BA, BH, CA, but decreased activity on CC relative to EnlA. CC is an important butyrate-producing bacteria with known beneficial effects on human health[16] . The chimera EAD2-

CBD2 was also interesting because it had similar overall activity and specificity to EnlA but was completely inactive on CA, a microbe associated with reduced risk of colon cancer[17]

We used linear regression analysis to estimate how each domain contributes to activity on each of the four human gut commensal species (Fig. 1d, supplementary Fig. 1). Chimeras with EAD1 and EAD2 were active on BA, but those with EAD3 showed no activity. Similarly, CBD1 and CBD2 contribute to activity on BA, while CBD3 decreases activity. All tested chimeric lysins were active on BH and the strongest effects driving activity seem to arise from the CBD domains. For CA, almost all lysins were inactive except those with CBD1. CC looked very similar to BA with both EADs and CBDs contributing to activity. Based on these results, EAD3 seems highly specific for cleaving BH peptidoglycan. Additionally, activity on BH and CA is largely determined by CBDs, while activity on BA and CC is determined by both EADs and CBDs.

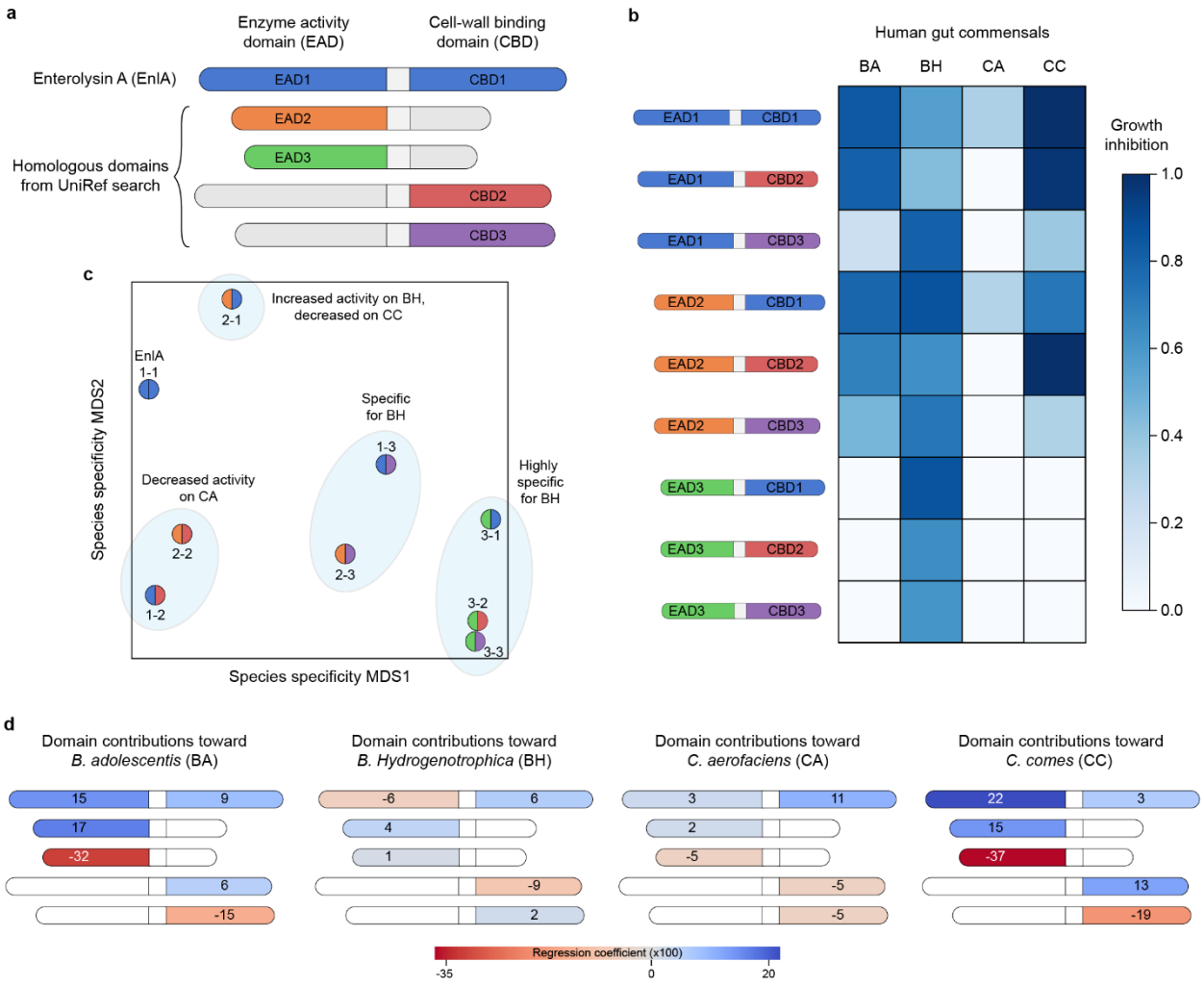

Figure 2.1. Design and screening of chimeric lysins. (a) Lysins consist of enzyme activity domains (EADs) and cell-wall binding domains (CBDs). We identified a diverse set of three EADs and three CBDs that can be shuffled to generate nice chimeric lysins. (b) We screened all nine chimeric lysins against a panel of four human gut commensal species. Growth inhibition was calculated by comparing the calculating the area under the growth curves (AUCs) for lysin and no lysin samples. (c) Visualization of each chimeric lysins specificity profile from panel b. We used multidimensional scaling (MDS) to reduce the 4-dimensional space to 2D for visualization. Each lysin is colored according to its constituent domains. The lysins cluster into distinct groups based on their specificity. (d) We used linear regression to estimate how each domain contributes to activity on each species. The domains are organized according to the layout in panel a. Blue colors indicate increased activity, while red colors indicate reduced activity.

2.3 Quantitative assessment of lysin activity against individual members of a synthetic community

The screening experiments in the previous section were performed with *E. coli* lysates and thus did not control for the absolute lysin concentration. We wanted to obtain more quantitative activity measurements to understand how lysin concentration affects growth inhibition across microbial species. We focused on EnlA (EAD1-CBD1) and the chimera Ch2-2 (EAD2-CBD2) due to their high expression and broad activity. We evaluated these two lysins on a diverse mix of fast growing, slow growing, and butyrate-producing microbes that were chosen in a previous study[18]. These microbes include *Bifidobacterium adolescentis* (BA), *Coprococcus comes* (CC), *Anaerostipes caccae* (AC), *Eubacterium rectale* (ER), and *Roseburia intestinalis* (RI).

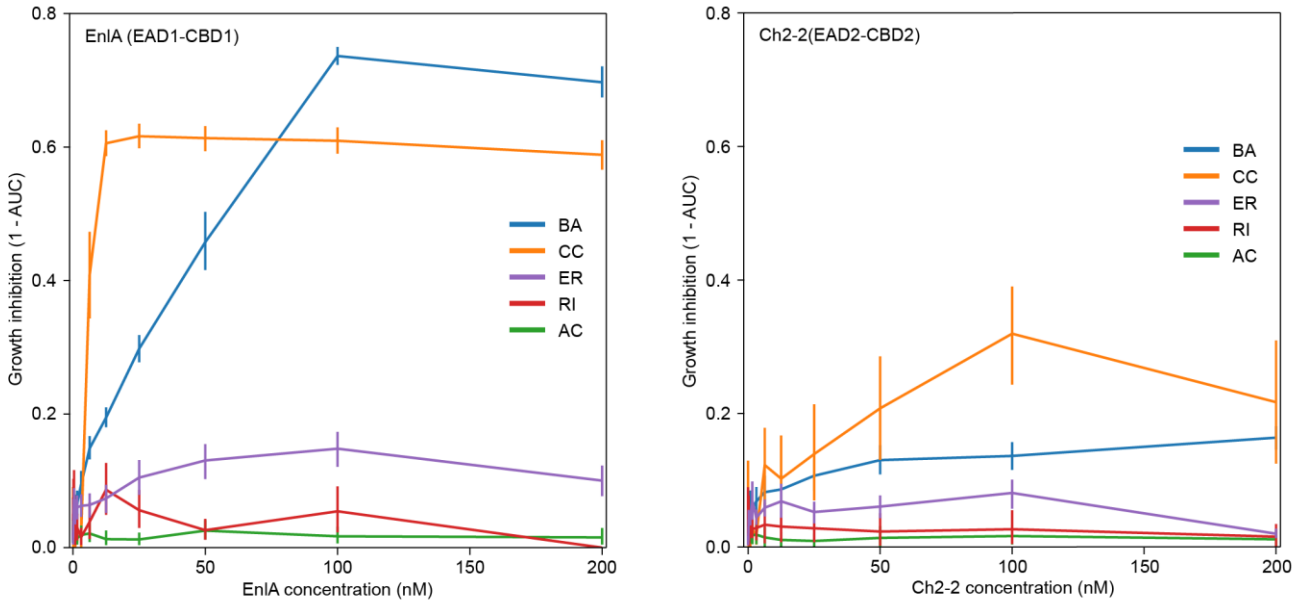

Figure 2.2. Quantitative titrations of lysins against single species. We titrated purified EnlA (top panel) and Ch2-2 (bottom panel) against monocultures of *Bifidobacterium adolescentis* (BA), *Coprococcus comes* (CC), *Anaerostipes caccae* (AC), *Eubacterium rectale* (ER), and *Roseburia intestinalis* (RI). Growth inhibition was calculated by comparing the calculating the area under the growth curves (AUCs) for lysin and no lysin samples.

We titrated purified lysins against single strains and calculated each microbe's relative growth at varying lysin concentrations (Fig. 2). EnlA showed strong growth inhibition against BA and CC, with maximum activity at 12.5nM and 100nM, respectively. EnlA showed moderate growth inhibition against AC with maximum activity at 100nM. Ch2-2 showed growth inhibition against BA, CC, and AC, but had overall lower activity relative to EnlA. At higher concentrations beyond 100nM, EnlA shows a preference for BA over CC, while Ch2-2 shows the opposite preference for CC over BA. Both EnlA and Ch2-2 had no activity against ER and RI. The quantitative differences and species preferences between EnlA and Ch2-2 will affect how they behave in a microbial community context.

2.4 Modulating the structure and function of synthetic gut microbiome communities

Microbial communities are rich ecosystems with many interdependent interactions that shape their behaviors. We wanted to test if our engineered lysins could modulate the structure and function of synthetic gut microbiome communities. We designed two synthetic communities based on a previous study[18] that result in stable coexistence between species and produce butyrate and other short-chain fatty acids. The first community (COM1) consists of BA and the three butyrate-producers CC, RI and ER. The second community (COM2) consists of BA and the three butyrate-producers CC, RI and AC.

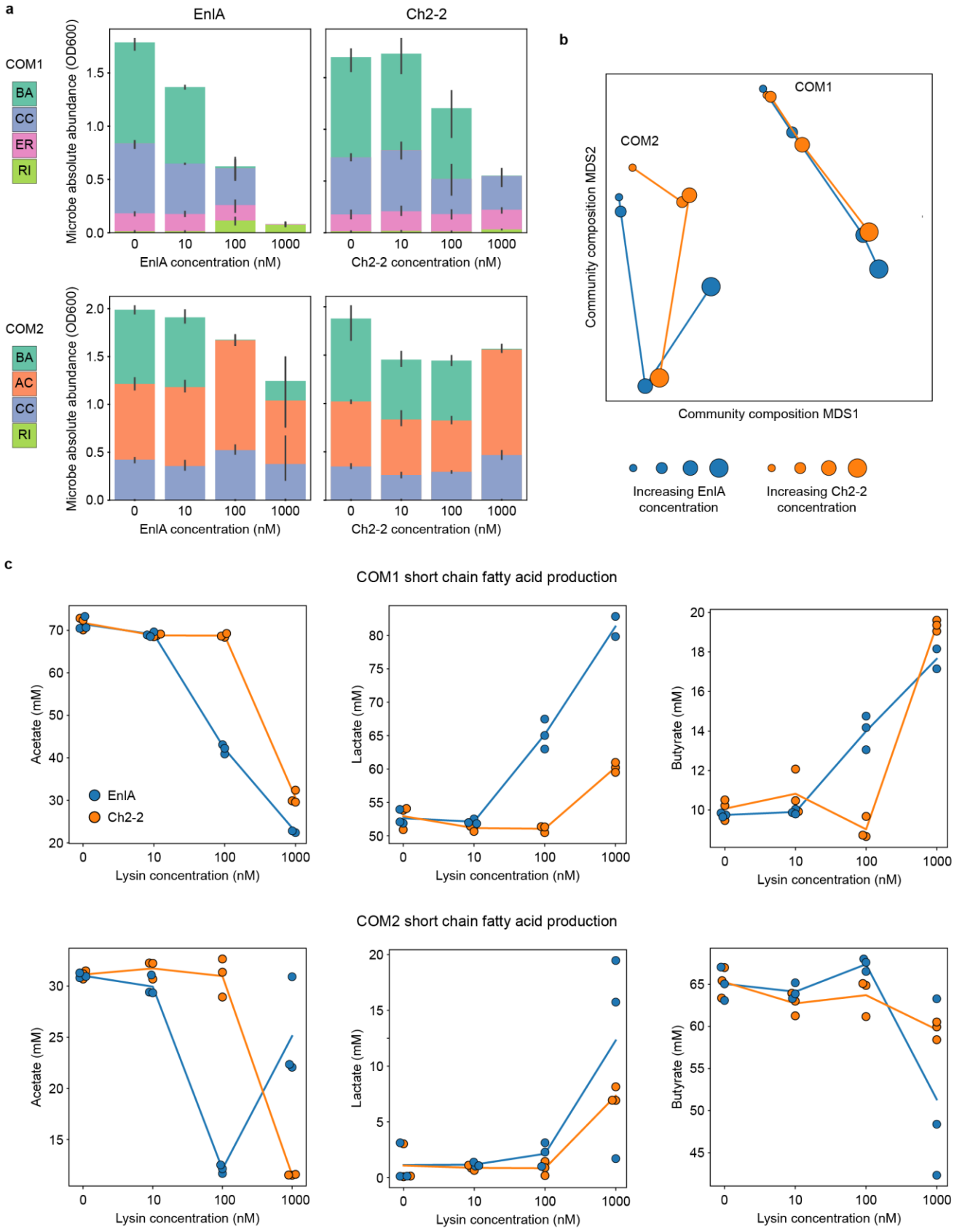
a
EnlA
Ch2-2
COM1
BA
CC
ER
RI
Microbe absolute abundance (OD600)
EnlA concentration (nM)
Ch2-2 concentration (nM)
COM2
BA
AC
CC
RI
b
COM1
COM2
Community composition MDS2
Community composition MDS1
Increasing EnlA concentration
Increasing Ch2-2 concentration
c
COM1 short chain fatty acid production
Acetate (mM)
Lactate (mM)
Butyrate (mM)
EnlA
Ch2-2
Lysin concentration (nM)
COM2 short chain fatty acid production

Figure 2.3. Modulating synthetic gut microbiome communities. (a) The community composition of COM1 (top row) and COM2 (bottom row) in response to increasing lysin concentrations. The bars represent absolute abundance of each microbe and the community experiments were performed in triplicate. (b) We visualized the response of COM1 and COM2 to increasing lysin concentrations using multidimensional scaling (MDS). The full five-dimensional community (BA, CC, EM, RI, and AC) was reduced to two dimensions. Increasing point size corresponds to increasing lysin concentration. (c) Short-chain fatty acid production of COM1 (top row) and COM2 (bottom row) at varying lysin concentrations. Each community was analyzed with three biological replicates shown as individual points and the lines correspond to the mean fatty acid concentration.

We tested the response of synthetic communities COM1 and COM2 to both lysins EnlA or Ch2-2 and measured abundance of each microbe and the quantity of short chain fatty acids produced. Increasing lysin concentration generally caused a decrease in overall community density but affected each microbial species differently (Fig. 3a). In COM1, there was a marked decrease in the presence of BA and this seems to open a niche for the slow growing RI to expand at high EnlA concentrations. We also found CC was largely unchanged across lysin concentrations despite showing high growth inhibition in single species measurements (Fig 1 and Fig 2). In the community context, CC competes with BA and may be less affected by lysins that preferentially lyse BA. 1000nM EnlA causes complete collapse of COM1, reducing both the community density and diversity. We found COM2 is less affected by lysins, and this seems to be a result of AC having minimal lysin sensitivity. Overall, we see microbes in the community context are less affected by lysins than in single-species experiments.

We performed multidimensional scaling (MDS) on the community composition to visualize how lysins reshape the community structure (Fig. 3b). We found COM1 and COM2 occupy distinct regions in community space and increasing lysin concentration causes

directional changes in the community composition. EnlA and Ch2-2 affect COM1 in a similar direction, but Ch2-2 requires ~10x more protein to achieve a similar effect to EnlA. EnlA and Ch2-2 have more varied effects on COM2, with the lower lysin concentrations moving the communities in different directions. We also measured the short chain fatty acids produced by the communities (Fig. 3c). For COM1, both lysins substantially decreased acetate levels, while increasing both lactate and butyrate. 1000nM Ch2-2 nearly doubled the buyrate produced by COM1. For COM2, both lysins decreased acetate, increased lactate, and slightly decreased butyrate. These results demonstrate how small quantities of lysins can drastically alter the structure and function of microbial communities.

2.6 Discussion

The human gut microbiome plays essential roles in human health and disease, and strategies to modulate and control this complex ecosystem could be used as therapeutics. Our work demonstrated the ability of lysins to target diverse human gut commensal bacteria, how domain recombination can give rise to chimeric lysins with altered species preferences, and how engineered lysins can directly remodel the structure and function of microbial communities. Lysins provide a general platform that can be rapidly tailored through protein engineering to control complex microbial ecosystems.

Our work is the first example using lysins to remodel the gut microbiome. Other targeted methods gut microbiome manipulation include prebiotics[19,20], probiotics[21], antimicrobials[22], and phage therapy[23]. These approaches have limited potential to specifically target a subset of microbes and tend to more broadly modulate the gut

microbiome from a dysbiosis state into a healthy state. Lysins offer two levels of specificity, occurring at the CBD and EAD, and thus provide tunable specify from narrow to broad. One challenge in applying lysins and other antimicrobials to control microbiomes is it's not clear a priori which microbes should be targeted to achieve a desired microbiome state. Interspecies interactions within a community give rise to complex behaviors that are difficult to predict.

There are many previous examples engineering lysins to target diverse bacterial species and treat bacterial infections. For example, work done by Gerstmans et al. developed a lysin domain shuffling and screening platform capable of creating lysins that target multiple strains of the gram-negative pathogen *A. bumanii*[24]. Other work shuffled lysin domains to target Gardella biofilms for treating and preventing bacterial vaginosis[25]. Lysins can additionally be fused to outer membrane permeabilizing (OMP) peptides to bypass the outer membrane and target gram-negative bacteria[24,26]. The modular structure and broad species range of lysins makes them ideal scaffolds for selectively targeting diverse microbial species.

The EnlA and Ch2-2 lysins showed potent activity to modulate the species structure of the synthetic human gut communities COM1 and COM2. These changes in species composition greatly influenced the short-chain fatty acid (SCFA) metabolite pools. Overall, the lysins reduced acetate, while increasing lactate and butyrate, all of which could have beneficial effects on the host. Microbially produced acetate is known to activate the parasympathetic nervous system, promoting ghrelin secretion and glucose-stimulated insulin secretion, resulting in hyperlipidemia, fatty liver disease, insulin

resistance and obesity[27]. Lactate is known to promote gut microbial diversity and gut health through anti-inflammatory and immunomodulatory effects[28]. Butyrate is a primary energy source for colonocytes, promotes a healthy gut barrier, limits pro-inflammatory cytokines, and inhibits oncogenic pathways[29].

We tested our engineered lysins in synthetic gut communities *in vitro*, but we would ultimately want to deliver lysins to the human gut. Oral delivery of proteins presents challenges with passing through the proteolytic and the acidic environment of the digestive tract. We envision engineering probiotic bacteria that secrete lysins and could be delivered orally. These probiotics could include *E. coli* Nissle 1917, lactobacillus, and bacteroides. Engineered probiotic bacteria could reside in the human gut for short or long timeframes and deliver designed lysins directly to the gastrointestinal tract.

Precisely controlling the structure, function, and behavior of the human gut microbiome will create a revolution in medicine and how we treat human disease. This level of control requires a comprehensive understanding of the interactions within and between the microbiome, the host, and the metabolome, and specific control knobs that alter the microbiome in a predictable manner. Furthermore, the microbiome states associated with human health are largely individual-specific and may require personalized microbiome therapies[25]. Lysins and other antimicrobial peptides/proteins provide a framework for targeted modulation of complex microbial ecosystems *in situ* and can be rapidly engineered to tailor the microbiome toward human health.

2.7 Methods

Bioinformatics search for lysin EAD and CBD domains

The sequence of wild-type enterolysin A (EnlA) was separated into EAD and CBD at the previously identified TP-rich linker at positions 181-194. These domains were then independently queried using jackhmmer[30] against the Uniref100 database to identify distant homologous domains. Query results were further processed by setting cutoffs of less than 70% pairwise identity and over 80% sequence coverage to the query sequence. This was done to ensure complete domains were selected and that they were sufficiently different from the query sequence and to each other. All domains identified that met the filtering criteria were submitted to InterPro for domain classification. For domains that were successfully classified by InterPro, their sequences were further analyzed to confirm the presence of relevant protein family motifs.

Lysin cloning and protein expression

Enterolysin A and other homologous domain genes were ordered as Gblocks (IDT). All gene inserts were created by PCR with appropriate GoldenGate adapters to such that all possible domain combinations could be assembled. Inserts were cloned using Golden Gate cloning with BsaI (NEB) into a pET22 plasmid. Plasmids were transformed into E. coli DH5 alpha and sequenced confirmed by Sanger sequencing through Functional Biosciences.

For expression of the assembled lysins, plasmids were transformed into E. coli BL21 (DE3). Starter cultures were made by inoculating from glycerol stocks into 5mL of LB

medium containing 100µg/mL Carbenicillin and cultured overnight at 37˚C and 250 rpm. 500µL of starter cultures were used to inoculate 50mL of Terrific broth in 250mL baffled flasks. Cultures were grown at 37˚C at 250rpm to an OD600 of ~0.6. Protein expression was induced with 50µM IPTG, and cultures were transferred into a pre-chilled shaker at 20˚C and grown for 18 hours at 250rpm. Cultures were then harvested by centrifugation in a tabletop centrifuge at 3000xG for 10 minutes at 4˚C.

Growth inhibition assays

All experiments were preceded by thoroughly sterilizing the workspace and material with spore-klenz and subsequently with 70% ethanol to avoid contamination of bacteria and bacterial spores. For each experiment, precultures of each species were prepared by thawing a single-use glycerol stock and combining the inoculation volume and media to a total volume of 10 mL until the stationary phase was reached at 37˚C. Incubation times are also listed in Supplemental Table 1. The OD600 values of the precultures were measured (Tecan F200 Plate Reader, 200 µL in 96-Well Microplate) and used to normalize each culture to an OD600 of 0.0066 by spinning down at 3200 x g for 10 min and resuspending with DM38. E coli lysate containing expressed lysins was prepared by pelleting the expression culture at 3,000xg for 5 minutes, discarding the supernatant, and resuspending in 1x PBS (137 mM NaCl, 2.7 mM KCl, 10 mM Na2HPO4, 1.8 mM KH2PO4) at 1/10 of the culture volume. Resuspended cultures were then lysed by sonication (5 seconds on 15 seconds off for a total on time of 1 minute. Sonicated samples were centrifuged at 4,000xg at 4˚C for 30 minutes and the soluble fraction was

transferred into conical tubes and stored on ice for temporary storage. Samples and controls were prepared by adding concentrated lysate to normalized pre-culture in 96-well plates to a final volume of 200µL. Concentrated empty-plasmid lysate was used as controls for each strain tested and each condition was done in triplicate. Plates were then sealed using semi-permeable membranes (Breathe-Easy seal Sigma-Aldrich) and placed on a microplate reader (Tecan F200 Plate Reader). OD600 was then monitored for 24-48 hours, for fast and slow growing strains respectively and shown in Table 1, at 37˚C in a plate reader. With the data obtained we calculated growth inhibition for each sample following the equation:

Equation 2.1. Growth inhibition formula for growth curves

$$growth\ inhibition = 1 - \left({AUC_{lysin}}/{AUC_{untreated}}\right)$$

Where AUC_{lysin} is the area under the growth curve for the lysin treated sample and $AUC_{untreated}$ is the under the growth curve for the untreated sample. Ridge regression was performed on the growth inhibition results using RidgeCV method with default parameters from the scikit-learn library in Python3 to estimate the domain contributions to growth inhibition.

For single strain titrations, each purified protein was first diluted to 2µM in 100mM Tris/HCl, 150mM NaCl pH 8.0 buffer. Then a 2-fold series dilution was performed such that final assay concentrations were 200nM, 100nM, 50nM, 25nM, 12.5nM, 6.25nM and

3.125nM, including a 0nM buffer negative control. All samples and control conditions were done in triplicate.

Protein purification

Cells were grown at 37˚C, 250RPM, to OD600 0.55-0.65 and induced with 100μM IPTG. Induced cultures were then grown at 30˚C, 250RPM, for 14-16 hours. After induction growth, cells were harvested by centrifugation at 3000xG, and the supernatant was discarded. Cell pellets were resuspended in 100mM Tris/HCl, 150mM NaCl pH 8.0, and lysed by sonication (5 seconds on, 15 seconds off, total sonication time 1 minute). Cell lysates were clarified by centrifugation at 4,000xG for 1 hour. Strep-tagged clarified lysates were purified by passing through a gravity column with Strep-tactin Sepharose resin (IBA), and proteins were eluted using 100mM Tris/HCl, 150mM NaCl, 2.5 mM desthiobiotin, and analyzed by SDS-PAGE. Buffer exchange was performed by dialyzing overnight in 100mM Tris/HCl and 150mM NaCl and was concentrated using 30kDa MW (Vivaspin) protein concentrator columns 30kDa MW. Stocks were aliquoted, flash-frozen in liquid nitrogen, and stored at -80˚C. Protein concentrations were determined using a Bradford assay from fresh, concentrated stock.

Strain Maintenance and anaerobic culture conditions

All anaerobic culturing was carried out in an anaerobic chamber (Coy Labs) with an atmosphere of 2.5 ± 0.5% H2, 15 ± 1% CO2, and balance N2. All prepared media, stock solutions, and materials were placed in the anaerobic chamber and left overnight to equilibrate. The strains used in this work were obtained from the sources listed in

Supplementary Data 1, and permanent stocks of each were stored in 25% glycerol at −80 °C. Batches of single-use glycerol stocks were produced for each strain by first growing a culture from the permanent stock in anaerobic basal broth (ABB) media (HiMedia or Oxoid) to stationary phase, mixing the culture in an equal volume of 50% glycerol and aliquoting 400 µL into Matrix Tubes (ThermoFisher) for storage at −80 °C. Quality control for each batch of single-use glycerol stocks included (1) plating a sample of the aliquoted mixture onto LB media (Sigma-Aldrich) for incubation at 37 °C in ambient air to detect aerobic contaminants and (2) Illumina sequencing of 16S rDNA isolated from pellets of the aliquoted mixture to verify the identity of the organism.

Community culturing and lysin titration

All experiments were preceded by thoroughly sterilizing the workspace and material with spore-klenz and subsequently with 70% ethanol to avoid contamination of bacteria and bacterial spores. For each experiment, precultures of each species were prepared by thawing a single-use glycerol stock and combining the inoculation volume and media (make a list for each strain) to a total volume of 10 mL until the stationary phase was reached at 37˚C. Incubation times are also listed in Table 1. The OD600 values of the precultures were measured (Tecan F200 Plate Reader, 200 µL in 96-Well Microplate) and used to normalize each culture to an OD600 of 0.0066 by spinning down at 3200 x g for 10 min and resuspending with DM38.

The tested communities were combined in a 96 deep-well plate by mixing equal volumes of each species' diluted preculture. Lysins were added to the communities to final concentrations of 0, 0.01, 0.1, and 1 uM. The 96 deep well plate was covered with a semi-

permeable membrane and incubated at 37 °C for 48 h. After the incubation, 20 uL of each sample was diluted in 96-Well Microplate with 180 uL PBS buffer for OD600 measurement. 200 µL of each sample was transferred to a new 96DW plate and pelleted by centrifugation at 3200×g for 10 min. 180 uL of each supernatant was removed from each sample and stored at −20 °C for subsequent metabolite quantification by high performance liquid chromatography (HPLC). The remaining cell pellets were stored at −80 °C for subsequent genomic DNA extraction for 16S sequencing.

HPLC quantification of organic acids

Supernatant samples were thawed at room temperature and added 2 µL of H2SO4. The samples were then centrifuged at 2400 × g for 10 min, and then 150 µL of each sample was filtered through a 0.2 µm filter using a vacuum manifold before transferring 70 µL of each sample to an HPLC vial. HPLC analysis was performed using either a ThermoFisher (Waltham, MA) Ultimate 3000 UHPLC system equipped with a UV detector (210 nm) or a Shimadzu HPLC system equipped with a SPD-20AV UV detector (210 nm). Compounds were separated on a 250 × 4.6 mm Rezex© ROA-Organic acid LC column (Phenomenex Torrance, CA) run with a flow rate of 0.2 mL min−1 and a column temperature of 50 °C. The samples were held at 4 °C before injection. Separation was isocratic with a mobile phase of HPLC grade water acidified with 0.015 N H2SO4 (415 µL L−1). At least two standard sets were run along with each sample set. Standards were 100, 20, and 4 mM concentrations of butyrate, succinate, lactate, and acetate. For most runs, the injection volume for both sample and standard was 25 µL. The resultant

data was analyzed using the Thermofisher Chromeleon 7 software package or the Shimadzu LabSolutions software package.

Genomic DNA extraction, DNA library preparation, sequencing, primer design, and data analysis

DNA extraction, library preparation, and sequencing were performed according to methods described in Clark 2021[18]. After experiments, cell pellets from 200 uL of culture were stored at -80C. Genomic DNA was extracted using a version of the DNeasy protocol (Qiagen) adapted for 96-well plates. Genomic DNA was normalized to 1 ng/μL in molecular-grade water and stored at -20˚C. Dual-indexed primers for multiplexed amplicon sequencing of the v3-v4 region of the 16S gene were designed as described previously and arrayed in 96-well, skirted PCR plates, using an acoustic liquid handling robot. Genomic DNA and PCR master mix were added to primer plates and amplified before sequencing on an Illumina MiSeq platform. Sequencing data were analyzed as described in Clark 2021[18]. In brief, basespace Sequencing Hub's FastQ Generation demultiplexed the indices and generated FastQ files. Paired reads were merged using PEAR (Paired-End reAd mergeR) v0.9.0[31]. Reads were mapped to a reference database of species used in this study, using the mothur v1.40.5 and the Wang method[32,33]. Relative abundance was, calculated by dividing the read counts mapped to each organism by the total reads in the sample. Absolute abundance was calculated by multiplying the relative abundance of an organism by the OD600 of the sample. Samples were excluded from further analysis if > 1% of the reads were assigned to a species not expected to be in the community (indicating contamination)

2.8 References

1. Fischetti, A. L. of B. P. V. A. Bacteriophage lysins as effective antibacterials. (2008).
2. Fischetti, V. A. Bacteriophage endolysins: A novel anti-infective to control Gram-positive pathogens. *Elsevier BV* vol. 300 357–362 (2010).
3. Fischetti, V. A. Exploiting what phage have evolved to control gram-positive pathogens. *Bacteriophage* **1**, 188–194 (2011).
4. Schmelcher, M. *et al.* Rapid Multiplex Detection and Differentiation of Listeria Cells by Use of Fluorescent Phage Endolysin Cell Wall Binding Domains. *Appl. Environ. Microbiol.* **76**, 5745–5756 (2010).
5. Obeso, J. M., Martínez, B., Rodríguez, A. & García, P. Lytic activity of the recombinant staphylococcal bacteriophage PhiH5 endolysin active against Staphylococcus aureus in milk. *Int. J. Food Microbiol.* **128**, 212–218 (2008).
6. Gerstmans, H., Criel, B. & Briers, Y. Synthetic biology of modular endolysins. *Elsevier BV* vol. 36 624–640 (2018).
7. Rodríguez-Rubio, L. *et al.* DUF3380 Domain from a Salmonella Phage Endolysin Shows Potent N-Acetylmuramidase Activity. *Appl. Environ. Microbiol.* **82**, 4975–4981 (2016).
8. Catalão, M. J., Milho, C., Gil, F., Moniz-Pereira, J. & Pimentel, M. A Second Endolysin Gene Is Fully Embedded In-Frame with the lysA Gene of Mycobacteriophage Ms6. *PLoS ONE* **6**, e20515 (2011).
9. Lee, K. O. *et al.* Structural Basis for Cell-Wall Recognition by Bacteriophage PBC5 Endolysin. *Structure* (2019) doi:10.1016/j.str.2019.07.001.
10. Ganguly, J., Low, L., Kamal, N., & others. The secondary cell wall polysaccharide of Bacillus anthracis provides the specific binding ligand for the C-terminal cell wall-

binding domain of two phage endolysins, PlyL and PlyG. *Glycobiology* **23**, 820–832 (2013).

11. Percy, M. & Gründling, A. Lipoteichoic acid synthesis and function in gram-positive bacteria. *Annu. Rev. Microbiol.* **68**, 81–100 (2014).
12. Walter, J. *et al.* D-alanyl ester depletion of teichoic acids in Lactobacillus reuteri 100-23 results in impaired colonization of the mouse gastrointestinal tract. *Environ. Microbiol.* **9**, 1750–1760 (2007).
13. Fabretti, F. *et al.* Alanine Esters of Enterococcal Lipoteichoic Acid Play a Role in Biofilm Formation and Resistance to Antimicrobial Peptides. *Infect. Immun.* **74**, 4164–4171 (2006).
14. Vélez, M. *et al.* Functional Analysis of d-Alanylation of Lipoteichoic Acid in the Probiotic Strain Lactobacillus rhamnosus GG. *Appl. Environ. Microbiol.* **73**, 3595–3604 (2007).
15. Fischetti, V. A. Phage Lysins: Novel Alternative to Antibiotics. in *Phage Therapy: A Practical Approach* (Springer, 2019). doi:10.1007/978-3-030-26736-0_12.
16. Notting, F., Pirovano, W., Sybesma, W. & Kort, R. The butyrate-producing and spore-forming bacterial genus *Coprococcus* as a potential biomarker for neurological disorders. *Cambridge University Press* vol. 4 (2023).
17. Moore, W. & Moore, L. Intestinal floras of populations that have a high risk of colon cancer. *Appl. Environ. Microbiol.* **61**, 3202–3207 (1995).
18. Clark, R. L. *et al.* Design of synthetic human gut microbiome assembly and butyrate production. *Nature Portfolio* vol. 12 (2021).

19. Olas, B. Probiotics, prebiotics and synbiotics-a promising strategy in prevention and treatment of cardiovascular diseases? *Int. J. Mol. Sci.* **21**, 1–15 (2020).
20. Chassard, C. & Lacroix, C. Carbohydrates and the human gut microbiota. *Curr. Opin. Clin. Nutr. Metab. Care* **16**, 453–460 (2013).
21. Hill, C. *et al.* Expert consensus document: The international scientific association for probiotics and prebiotics consensus statement on the scope and appropriate use of the term probiotic. *Nat. Rev. Gastroenterol. Hepatol.* **11**, 506–514 (2014).
22. Chen, P. B. *et al.* Directed remodeling of the mouse gut microbiome inhibits the development of atherosclerosis. vol. 38 1288–1297 (2020).
23. Lee, H. *et al.* Targeted Approaches for In Situ Gut Microbiome Manipulation. *Genes (Basel)* vol. 9 351–351 (2018).
24. Gerstmans, H. *et al.* A VersaTile-driven platform for rapid hit-to-lead development of engineered lysins. vol. 6 (2020).
25. Landlinger, C. *et al.* Engineered Phage Endolysin Eliminates Gardnerella Biofilm without Damaging Beneficial Bacteria in Bacterial Vaginosis Ex Vivo. *MDPI AG* vol. 10 54 (2021).
26. Defraine, V. *et al.* Efficacy of artilysin art-175 against resistant and persistent acinetobacter baumannii. vol. 60 3480–3488 (2016).
27. Perry, R. J. *et al.* Acetate mediates a microbiome–brain–β-cell axis to promote metabolic syndrome. *Nature* **534**, 213–217 (2016).
28. De Filippis, F., Pasolli, E. & Ercolini, D. The food-gut axis: lactic acid bacteria and their link to food, the gut microbiome and human health. *FEMS Microbiol. Rev.* **44**, 454–489 (2020).

29. Singh, V. *et al.* Butyrate producers, “The Sentinel of Gut”: Their intestinal significance with and beyond butyrate, and prospective use as microbial therapeutics. *Front. Microbiol.* **13**, (2023).
30. Johnson, L. S., Eddy, S. & Portugaly, E. Hidden Markov model speed heuristic and iterative HMM search procedure. *BMC Bioinformatics* **11**, 431–431 (2010).
31. Zhang, J., Kobert, K., Flouri, T. & Stamatakis, A. PEAR: a fast and accurate Illumina Paired-End reAd mergeR. *Bioinformatics* **30**, 614–620 (2014).
32. Schloss, P. D. *et al.* Introducing mothur: open-source, platform-independent, community-supported software for describing and comparing microbial communities. *Appl. Environ. Microbiol.* **75**, 7537–7541 (2009).
33. Wang, Q., Garrity, G. M., Tiedje, J. M. & Cole, J. R. Naive Bayesian classifier for rapid assignment of rRNA sequences into the new bacterial taxonomy. *Appl. Environ. Microbiol.* **73**, 5261–5267 (2007).

Chapter 3: Degradation of gut trimethylamine(TMA) with trimethylamine dehydrogenase(TMADH)

3.1 Enzymatic degradation of harmful metabolites in the gut.

Although several other approaches for gut microbiome therapies have been previously discussed, they mainly center around introducing beneficial microbes, healthy complex communities with keystone species, or remodeling microbial composition. However, an alternative strategy could be to directly target and degrade harmful metabolites produced by gut microbes. In this approach rather than promoting the production of beneficial metabolites, the aim is to remove harmful metabolites through enzymatic degradation within the gut directly. One potential target metabolite for this approach is trimethylamine(TMA), which in oxidized form as trimethylamine-n-oxide (TMAO) is a marker for development of CVD[1].

Specific gut bacteria are responsible for the conversion of choline and other methylamines into TMA. These bacteria include members of the Firmicutes phylum, which have been associated with higher TMA production[2,3]. Once produced, TMA is absorbed into the bloodstream and transported to the liver, where it is converted to trimethylamine-N-oxide (TMAO) by flavin-containing monooxygenases[4]. TMAO has been used as a marker for the development of obesity[5,6], and cardiovascular disease[7,8], possibly due to shifts in gut microbial composition favoring TMAO-producing bacteria[9]. Reducing the levels of TMAO in the body could, therefore, have beneficial effects on cardiovascular health.

Other alternative for strategies for controlling TMAO levels include reducing precursor intake (e.g. choline and carnitine), inhibiting microbial TMA production, or manipulating the FMO3 enzyme that catalyzes TMA to TMAO conversion.

3.2 Trimethylamine dehydrogenase: a trimethylamine degrading enzyme

Trimethylamine dehydrogenase (TMADH) is an iron-sulfur flavoprotein that catalyzes the oxidative demethylation of trimethylamine to form dimethylamine and formaldehyde. It is composed of two identical subunits, each containing three structural domains. The largest domain at the N-terminus is an eight-stranded parallel alpha/beta barrel containing a [4Fe-4S] cluster. The flavin mononucleotide (FMN) cofactor is covalently bound to the enzyme through a 6-S-cysteinyl FMN bond[10]. This bond is specifically linked to the amino acid residue cysteine at position C30 of the enzyme's polypeptide chain[11]. The enzymatic reaction follows a Ping-Pong mechanism where the substrate binds to the enzyme, leading to the reduction of the flavin mononucleotide (FMN) and subsequent electron transfer to the iron-sulfur cluster (Fig.4). This reduction requires electron-transferring flavoprotein (ETF) or an ETF analogue to complete the electron transfer process.

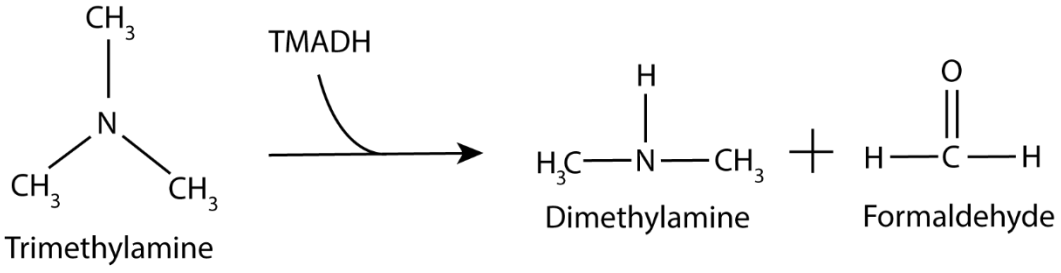

Figure 3.1. Degradation of trimethylamine by TMADH

Enhancing the activity of TMADH through protein engineering could potentially reduce TMA levels and consequently TMAO in the human body, and thus mitigate the development of cardiovascular disease. Since it remains untested under physiological conditions, functional screening methods are required for future engineering of this enzyme for gut microbiome applications.

3.3 Trimethylamine activity screening assay

Although many different approaches may be chosen for engineering and design, first viable methods for detecting trimethylamine dehydrogenase activity are required. If engineered and delivered to the gut, TMADH could degrade trimethylamine within the colon or gastrointestinal tract and thereby reduce the amount of trimethylamine available for conversion to TMAO.

The screening for activity was performed using ETF analogue previously used in stopped-flow spectroscopy studies of TMADH ferrocenium hexafluorophosphate (Fc+) (Fig. 3.2). By utilizing an Fc+, we aimed to avoid dual purification of future TMADH and ETF for adaptability into high throughput assays. Both control conditions showed no activity as expected. The sample TMADH+TMA is unable to perform turnovers since TMADH requires ETF to perform multiple turnovers. However, samples with all three TMADH, Fc+, and TMA present in the sample produced an average of 82uM formaldehyde from the initial 100uM in the sample.

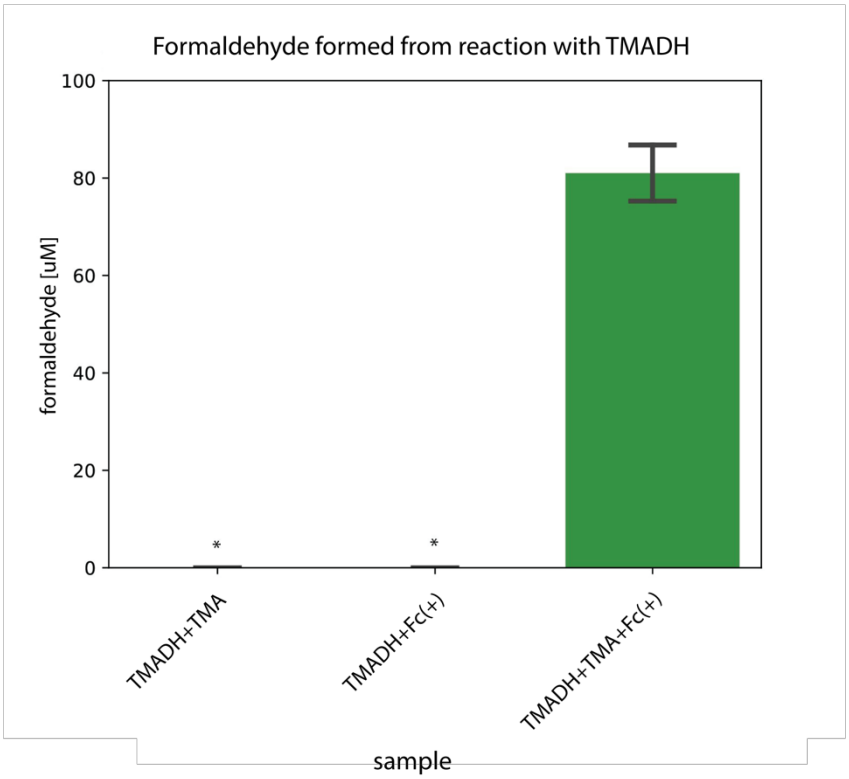

Figure 3.2. Detection of formaldehyde produced by TMADH mediated TMA degradation under aerobic conditions. Results show detection of formaldehyde produced as a degradation product of TMADH and ETF analogue Fc(+).

Fc+ was added in surplus at 250uM which may have contributed to a decrease in activity as overabundant Fc+ has been shown to decrease TMADH activity[12]. Another notable finding derived from these results is that TMADH can indeed work under aerobic conditions, as all other assays were explicitly performed under anaerobic conditions due to concerns over oxidation of the iron-sulfur cluster. This would allow for flexibility in handling and platform developed for high-throughput screening of TMADH variants.

3.4 Methods

Cloning expression and purification of trimethylamine dehydrogenase

The TMADH gene was cloned from a plasmid provided by Wenbo Lu from the Venturelli lab. The gene insert was created by PCR with appropriate GoldenGate

adapters and cloned using Golden Gate cloning with BsaI (NEB) into a pET22 plasmid containing an N-terminal strep-tag. Plasmids were transformed into E. coli DH5 alpha, dna harvested (DNA cleanup and concentration kit, Zymo Research) and sequenced confirmed by Sanger sequencing through Functional Biosciences.

Protein purification

Cells were grown at 37˚C, 250RPM, to OD600 0.55-0.65 and induced with 100μM IPTG. Induced cultures were then grown at 37˚C, 250RPM, for 3 hours. After induction growth, cells were harvested by centrifugation at 3000xG, and the supernatant was discarded. Cell pellets were resuspended in 100mM Tris/HCl, 150mM NaCl pH 8.0, and lysed by sonication (5 seconds on, 15 seconds off, total sonication time 1 minute). Cell lysates were clarified by centrifugation at 4,000xG for 1 hour. Strep-tagged clarified lysates were purified by passing through a gravity column with Strep-tactin Sepharose resin (IBA), and proteins were eluted using 100mM Tris/HCl, 150mM NaCl, 2.5 mM desthiobiotin, and analyzed by SDS-PAGE. Buffer exchange was performed by dialyzing overnight in 100mM Tris/HCl and 150mM NaCl and was concentrated using 30kDa MW (Vivaspin) protein concentrator columns 30kDa MW. Stocks were aliquoted, flash-frozen in liquid nitrogen, and stored at -80˚C. Protein concentrations were determined using a standard Bradford assay.

TMADH activity assays by formaldehyde detection

Formaldehyde detection assays were performed using a commercially available formaldehyde assay kit (MAK131 Sigma Aldrich). Solutions of TMA-HCl, DMA-HCl were

prepared at a concentration of 4uM with 0uM control. To deproteinate, 10% TCA was added to each sample, vortexed, and centrifuged at 14,000 rpm for 5 minutes. Samples were neutralized with an appropriate amount of Neutralizer following the protocol provided with the kit. Samples not used on the same day were stored at -80C. The standard curve was created by performing linear regression on samples of 0uM, 20uM, 40uM, 60uM, 80uM, and 100uM formaldehyde and measuring fluorescence intensity (FLU) at excitation and emission wavelengths of 370 nm and 470 nm, respectively.

To calculate the formaldehyde concentration, we used the standard curve plotted from the values obtained from the standards and applied linear regression to determine the slope. The formaldehyde concentration in the samples is calculated using the formula:

Equation 3.1. Formaldehyde concentration calculation from fluorescence measurements

$$formaldehyde\ [\mu M] = \frac{(FLU_{sample} - FLU_{blank}) - FLU_{water}}{slope} \times 1.875$$

where FLU_water is the value for the 0 standard, and 1.875 is the dilution factor for deproteinated samples.

3.5 Conclusions

Directly removing harmful metabolites could provide a strategy for gut microbiome therapies as an alternative to removing problematic endogenous microbes. Trimethylamine dehydrogenase engineering presents a potential approach to mitigate cardiovascular disease by directly reducing gut TMA levels. Our approach can accurately

measure TMA reduction in vitro and under aerobic conditions to serve as an early approach for engineering functional TMADH variants to improve TMA degradation. Although the degradation of trimethylamine by TMADH might be beneficial, its degradation product formaldehyde has the potential to further remodel the gut microbiome[13–16]. Further development is required to adapt the assays for higher screening throughput. Alternate electron acceptors, such as phenazine methosulfate, could also be explored to adapt these assays for higher throughput screening without the requirement of purified protein.

3.6 References

1. Swanepoel, I. *et al.* Trimethylamine N-oxide (TMAO): a new attractive target to decrease cardiovascular risk. *Postgraduate Medical Journal* **98**, 723–727 (2021).
2. Romano, K. A., Vivas, E., Amador-Noguez, D. & Rey, F. Intestinal Microbiota Composition Modulates Choline Bioavailability from Diet and Accumulation of the Proatherogenic Metabolite Trimethylamine-N-Oxide. *mBio* **6**, (2015).
3. Rath, S., Rud, T., Pieper, D. & Vital, M. Potential TMA-Producing Bacteria Are Ubiquitously Found in Mammalia. *Frontiers in Microbiology* **10**, (2020).
4. Fennema, D., Phillips, I. & Shephard, E. Trimethylamine and Trimethylamine N-Oxide, a Flavin-Containing Monooxygenase 3 (FMO3)-Mediated Host-Microbiome Metabolic Axis Implicated in Health and Disease. *Drug Metabolism and Disposition* **44**, 1839–1850 (2016).
5. Bi, S.-H. *et al.* Higher serum trimethylamine N-oxide (TMAO) levels are associated with increased visceral fat in hemodialysis patients. *Clinical Nephrology* (2023) doi:10.5414/CN111163.

6. Tang, W. & Hazen, S. Probiotic Therapy to Attenuate Weight Gain and Trimethylamine N-oxide (TMAO) Generation: A Cautionary Tale. *Obesity (Silver Spring, Md.)* **23**, 2321–2322 (2015).
7. Yang, S. *et al.* Gut Microbiota-Dependent Marker TMAO in Promoting Cardiovascular Disease: Inflammation Mechanism, Clinical Prognostic, and Potential as a Therapeutic Target. *Frontiers in Pharmacology* **10**, (2019).
8. Mens, T. E., Büller, H. & Nieuwdorp, M. Targeted inhibition of gut microbiota proteins involved in TMAO production to reduce platelet aggregation and arterial thrombosis: a blueprint for drugging the microbiota in the treatment of cardiometabolic disease? *Journal of Thrombosis and Haemostasis* **17**, 3–5 (2018).
9. Panda, S. S., Nayak, A., Shah, S. & Aich, P. A Systematic Review on the Association between Obesity and Mood Disorders and the Role of Gut Microbiota. *Multidisciplinary Digital Publishing Institute* vol. 13 488–488 (2023).
10. Sullivan, P. A. & Dickinson, F. M. The covalent structure of flavin in trimethylamine dehydrogenase from Bacterium aminophilum. *Biochemical Journal* **153**, 337–347 (1976).
11. Barber, M. J. *et al.* Assembly of redox centers in the trimethylamine dehydrogenase of bacterium W3A1. Properties of the wild-type enzyme and a C30A mutant expressed from a cloned gene in Escherichia coli. *Biochemistry* **31**, 3497–3504 (1992).
12. Husain, M., Barker, J. L., Merritt, A. H. & Green, G. H. Redox cycles in trimethylamine dehydrogenase and mechanism of substrate inhibition. *Journal of Biological Chemistry* **257**, 12329–12340 (1982).

13. Guo, J. *et al.* Exposure to Formaldehyde Perturbs the Mouse Gut Microbiome. *Genes* **9**, (2018).
14. Liu, K. & He, R. Gut Microbiota, Formaldehyde Dysmetabolism, and Cognitive Impairment. in *Research Progress on Environmental, Health, and Safety Aspects of Engineered Nanomaterials* 99–119 (2017). doi:10.1007/978-94-024-1177-5_6.
15. Williams, H. *et al.* Effects of dietary supplementation of formaldehyde and crystalline amino acids on gut microbial composition of nursery pigs. *Scientific Reports* **8**, (2018).
16. Chiu, K. K., Warner, G. R., Nowak, R., Flaws, J. & Mei, W. The Impact of Environmental Chemicals on the Gut Microbiome. *Toxicological Sciences* (2020) doi:10.1093/toxsci/kfaa065.

Chapter 4: Future directions

4.1 Lysins for gut microbiome remodeling

This work has presented the promising potential of engineered lysins as novel antimicrobials for gut microbiome remodeling. Several fundamental factors hinder further research through bottom-up approaches for engineering and testing lysins. Some of these factors include challenging in culturing stable complex gut microbiomes in-vitro, complex interspecies interactions that are still not well understood like host-microbiome interactions, and other unknown factors that contribute to stability and microbiome resilience. While lysins are extensively studied and engineered to target microbes, particularly MDR pathogenic microbes, the mechanisms underlying the functionality of lysin enzymatic domains and binding properties of binding domains relatively understudied.

To address the challenge of granular CBD engineering we developed a proof-of-concept approach to engineer CBDs to target a particular microbe of interest. By displaying a library of CBDs, paired with fluorescently tagging a microbe of interest with a fluorescent bacterial stain such as BacLight (Thermo Fischer Scientific), functional domains displayed on the yeast cell wall will bind to the microbe of interest. The principle of the approach is to design binding libraries, clone them into yeast, mix fluorescently tagged microbe of interest and use FACS for screening functional library variants (Figure 4.1a). Our approach used the wild-type enterolysin A CBD (enlA-CBD) for binding enterolysin A native target L. lactis. We found that non-CBD displaying yeast was incapable of binding *L. lactis* when mixed in PBS buffer while enlA-CBD displaying yeast was capable of binding *L. lactis* (Figure 4.1b). Under control conditions, EnlA-CBD displaying yeast could

bind BacLight Green (Thermo Fischer Scientific) tagged cells, while non-CBD displaying yeast were not (Figure 4.1c). We prepared a simulated library screening by preparing a mixture of 10% EnlA-CBD and 90% non-CBD displaying yeast within a single sample to perform one round of FACS enrichment. We saw an increase to 50% EnlA-CBD fraction in the sorted samples from the initial 10% pre-sort samples (Figure 4.1d). This promising result shows significant enrichment in a single pass with a known CBD with a high affinity towards *L. lactis.* Further rounds of enrichment and other optimizations to this approach are required for its adaptability to different microbial strains. However, it provides a functional platform amenable to high-throughput engineering of CBD libraries, therefore aiding in the discovery of novel target-specific CBDs and potentially elucidating design principles for developing targeted CBDs.

A more comprehensive and integrated approach is required to address further challenges in lysin engineering. Integrating mechanistic studies of the enzymatic domains together with the multi-omics characterization of the microbiome response to lysin treatment can provide crucial insights for a more rational design of lysins optimized for microbiome remodeling. Studies revealing binding substrates for CBDs displayed in the cell wall of target bacteria would be beneficial for *in silico* and *in vitro* approaches to optimize lysin binding affinity and specificity for desired gut microbe targets. Therefore, library screening of binding domains using display technologies, such as our proposed approach, would inform on the binding specificity profiles and could further create functional lysins libraries for future community experiments, maximizing target specificity within a complex microbial environment.

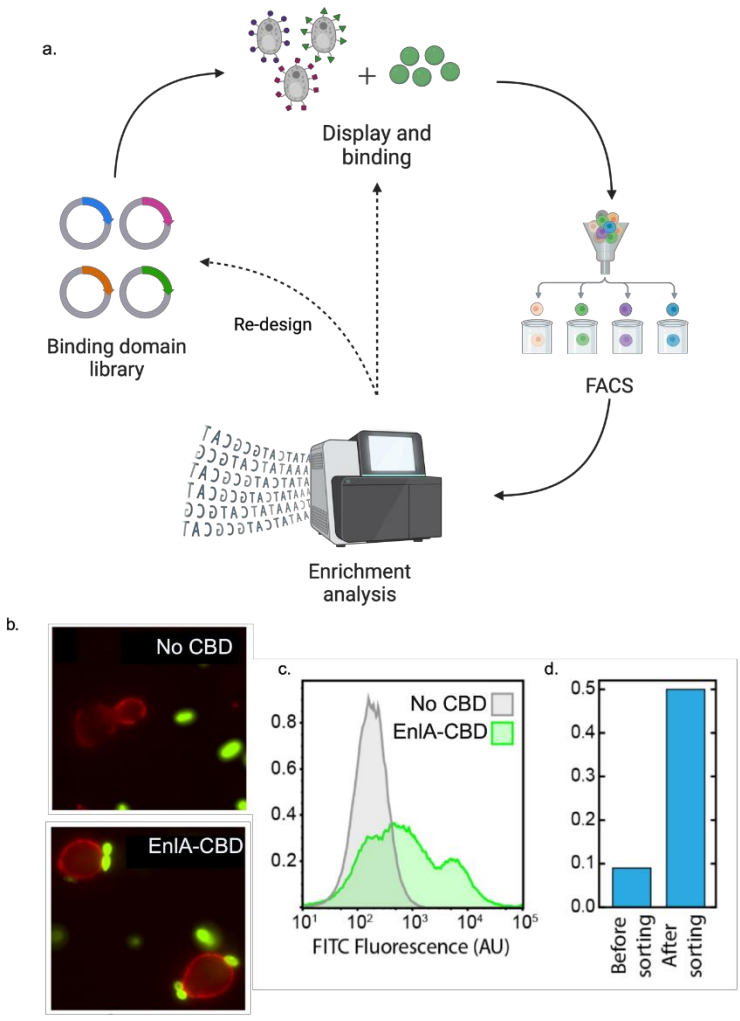

Figure 4.1. A FACS-based platform for the engineering of CBDs. General workflow for engineering CBDs with targeted binding (a). Conceptual workflow for developing novel CBDs with targeted specificity in the following procedure: 1. Creating CBD libraries and transforming them into yeast 2. Mixing the displaying yeast and tagged microbe of interest 3. Sorting by FACS 4. Performing enrichment analysis of functional variants. (b) Microscopy images of displaying yeast (red) tagged with anti-myc Alexa fluor 647 and BacLight Green stained L. lactis (green). Non-CBD-containing yeast don't show binding to the L. lactis (top), while EnlA-displaying yeast show consistent localization of several L. lactis cells on their surface (bottom).(c) Flow cytometry results for FITC fluorescence show biding of L. lactis for EnlA-CBD displaying yeast. (d) Pre- and post-sort fractions of positive control (EnlA-CBD) present in the samples.

As researchers continue to expand the repertoire of engineered lysins and elucidate the mechanisms underlying their specificity, this class of antimicrobials will become increasingly valuable as tools for remodeling the gut microbiome, novel antimicrobials, and studying complex microbiome dynamics as perturbation-causing agents

4.2 Enzymatic degradation of harmful metabolites

Practical approaches for harnessing enzymes to alter the gut metabolome are needed for a range of applications, from the treatment of metabolic diseases to mitigating

the effects of environmental exposures. Our work proposed using engineered enzymes to degrade or transform harmful small molecule metabolites in the gut. Careful consideration of the functional and compositional changes in the gut microbiome following enzymatic interventions is required, considering the effect of reaction products on the gut microbiome. For TMADH, it means further assessing whether the production of formaldehyde would significantly impact the gut microbiome diversity and metabolic function and if the metabolic capacity of the microbiome is compromised.

4.3 Current challenges and limitations

There are several challenges for these gut microbiome therapies to be developed in a systematic and predictable manner. One such limitation is our inability to culture and maintain complex microbial communities that resemble real communities. This is due to gaps in knowledge of host-microbiome interactions, nutrient requirements or microbe-microbe interactions that maintain stable communities under physiological conditions. There have been several approaches of creating bioreactors capable of sustaining complex gut microbiome communities inoculated from real samples of complex microbiomes[1–5]. However, all have been incapable of maintaining such communities without introducing major biases in composition which ultimately alter overall microbiome metabolism[6]. Furthermore, in-vitro studies are also highly media dependent and creating stable communities from individual gut isolates remains a challenging and empirical endeavor. Thus, creating controllable and predictable stable communities over time from individual gut isolates is largely limited to microbes for which interactions are well defined and community specific protocols have been established, culturable gut microbiome isolates, and empirically tested combinations of gut isolates that can replicate metabolic

function for SCFA or metabolite production in general. Further challenges arise when considering what features make up a healthy microbiome. Specific healthy states of the gut microbiome are highly variable and individual specific, largely depend on region, diet, upbringing and several other factors.

4.4 Methods

Plasmids and bacterial cultures

We adapted a pYD1 plasmid, provided by Eric Shusta's laboratory, by PCR to serve as a GoldenGate backbone (pYD1-GG) for cloning in the EnlA-CBD gene. The negative control (No-EAD) plasmid was prepared by circularizing the adapted pYD1-GG linear backbone such that the myc-tag was kept, but no binding domain remained at the C-terminus. The EnlA-CBD gene insert was created by PCR out of our EnlA gene plasmid (Appendix A.3) with appropriate Golden Gate adapters and cloned into our pYD1-GG backbone. Plasmids were transformed into E. coli DH5α(DE3), plated into LB agar plates, and placed in an incubator to grow overnight at 37ºC. Single colonies were picked from the plate, inoculated into 5mL of LB media with carbenicillin and placed in an incubator to grow overnight at 37ºC with shaking. After overnight growth in media, they were DNA harvested (DNA cleanup and concentration kit, Zymo Research) and sequence confirmed by Sanger sequencing through Functional Biosciences. *L. lactis subsp. cremoris mg1363* was provided by the van Pijkeren laboratory. *L. lactis* was inoculated into 5mL of MG17 media from single overnight colonies and grown overnight at room temperature.

Yeast display

Both negative and positive control plasmids were cloned into *S. cerevisiae* strain EBY100 following a previously published protocol[7]. Overnight precultures were prepared by inoculating a single colony into 5 mL of SDCAA media and incubating overnight at 30˚C with shaking. Precultures were inoculated into SDCAA media and diluted to an OD_{600} of 0.2. Cells were then grown at 30˚C with shaking for 4-6 hours until their OD_{600} reached 1.0. Cells were then pelleted by centrifugation at 3000xG for 5 minutes, washed with PBS, resuspended in 5mL of SGCAA media to induce display, and grown overnight at 20˚C with shaking.

Preparation of samples and FACS analysis

All displaying yeast and *L. lactis* samples were prepared fresh before sorting experiments. Yeast samples were pelleted by centrifugation, washed twice, and resuspended to a final OD_{600} of 1.0. Yeast samples were then tagged with the anti-c-myc Alexa fluor 647 (Sigma-aldrich) according to the manufacturers protocol. *L. lactis* samples were pelleted by centrifugation and resuspended to an OD_{600} of 1.0 in PBS. Negative control samples contained only non-CBD displaying yeast mixed with *L. lactis* samples at 1:10 ratio yeast to *L. lactis*. For the positive control, pre-normalized non-CBD and EnlA-CBD yeast samples were mixed at a ration of 1:9 non-CBD to EnlA-CBD yeast. This control was then mixed with *L. lactis* at a 1:10 ratio yeast to *L. lactis*. All sorting done was performed using a Sony SH800S cell sorter with a 70μM sorting chip.

Enrichment results analysis

Sorting results were obtained by outgrowing sorted samples in SDAA media with carbenicillin to allow growth of yeast cells while preventing *L. lactis* growth. Samples were then DNA extracted using a Zymoprep Yeast Plasmid Miniprep kit (Zymo Research) and normalized to 20ng/μL. Each DNA sample was amplified by PCR targeting the EnlA-CBD flanking regions. Image analysis of an agarose gel from the PCR products was performed using MATLAB R13, measuring peak intensity of the amplified bands and normalizing by subtracting the average intensity of the background.

4.5 References

1. Guzmán-Rodríguez, M. *et al.* Using bioreactors to study the effects of drugs on the human microbiota. *Methods* **149**, 31–41 (2018).
2. Habib, S., Swaby, A. M., Gaisawat, M. B., Kubow, S. & Agellon, L. A novel, scalable, and modular bioreactor design for dynamic simulation of the digestive tract. *Biotechnol. Bioeng.* **118**, 4338–4346 (2021).
3. Jin, Z., Ng, A., Maurice, C. & Juncker, D. The Mini Colon Model: a benchtop multi-bioreactor system to investigate the gut microbiome. *Gut Microbes* **14**, (2022).
4. Kumar, S., Wittmann, C. & Heinzle, E. Review: Minibioreactors. *Biotechnol. Lett.* **26**, 1–10 (2004).
5. Mendez, D. F. G., Sanabria, J., Wist, J. & Holmes, E. Effect of Operational Parameters on the Cultivation of the Gut Microbiome in Continuous Bioreactors Inoculated with Feces: A Systematic Review. *J. Agric. Food Chem.* (2023) doi:10.1021/acs.jafc.2c08146.

6. García Mendez, D. F., Sanabria, J., Wist, J. & Holmes, E. Effect of Operational Parameters on the Cultivation of the Gut Microbiome in Continuous Bioreactors Inoculated with Feces: A Systematic Review. *J. Agric. Food Chem.* (2023) doi:10.1021/acs.jafc.2c08146.
7. Boder, E. T. & Wittrup, D. K. Yeast surface display for screening combinatorial polypeptide libraries. *Nat. Biotechnol.* **15**, 553–557 (1997).

Appendix A: Gut microbiome isolate information, lysin genes, and media recipes

Table A.1. Strain information

Abbreviation	Species	Strain	Source	Type Strain?	Inoculum Volume (uL)	Preculture Media	Preculture Time (hr)
BAD	*Bifidobacterium adolescentis*	*Bifidobacterium adolescentis* E194a (Variant a)	Rey Lab	Yes	400	ABB	16
CAE	*Collinsella aerofaciens*	*Collinsella aerofaciens* VPI 1003 [DSM 3979]	DSMZ	Yes	400	ABB	40
ACA	*Anaerostipes caccae*	*Anaerostipes caccae* L1-92 [DSM 14662]	DSMZ	Yes	400	ABB	16
BHY	*Blautia hydrogenotrophica*	*Blautia hydrogenotrophica* S5a33 [DSM 10507]	DSMZ	Yes	400	ABB	40
ERE	*Eubacterium rectale*	*Eubacterium rectale* VPI 0990 [ATCC 33656]	ATCC	Yes	400	ABB	40
RIN	*Roseburia intestinalis*	*Roseburia intestinalis* L1-82 [DSM 14610]	DSMZ	Yes	400	ABB	40
CCO	*Coprococcus comes*	*Coprococcus comes* VPI CI-38	Rey Lab	Yes	400	ABB	16

Table A.2. DM38 Media Composition

Component	Concentration (mM)	Stock Solution
CaCl2	1.3	1000x Stock Solution of CaCl2, CuSO4, Pyrixodal, Thymidine
CuSO4	0.021	1000x Stock Solution of CaCl2, CuSO4, Pyrixodal, Thymidine
Pyrixodal	9.8E-03	1000x Stock Solution of CaCl2, CuSO4, Pyrixodal, Thymidine
Thymidine	0.021	1000x Stock Solution of CaCl2, CuSO4, Pyrixodal, Thymidine
Xanthine	0.025	1000x Stock Solution of Xanthine and Folic Acid
Folic Acid	2.4E-03	1000x Stock Solution of Xanthine and Folic Acid
Orotic Acid	0.064	100x Stock Solution of Orotic Acid
AlK(SO4)2	3.9E-03	100x Stock Solution purchased from Vendor (ATCC Mineral Mix)
Co(NO3)2	0.055	100x Stock Solution purchased from Vendor (ATCC Mineral Mix)
EDTA	0.17	100x Stock Solution purchased from Vendor (ATCC Mineral Mix)
FeSO4	0.066	100x Stock Solution purchased from Vendor (ATCC Mineral Mix)
H3BO3	0.016	100x Stock Solution purchased from Vendor (ATCC Mineral Mix)
MgSO4	2.7	100x Stock Solution purchased from Vendor (ATCC Mineral Mix)
MnSO4	0.33	100x Stock Solution purchased from Vendor (ATCC Mineral Mix)
Na2MoO4	4.9E-03	100x Stock Solution purchased from Vendor (ATCC Mineral Mix)
Na2SeO3	5.8E-04	100x Stock Solution purchased from Vendor (ATCC Mineral Mix)
Na2WO4	3.4E-03	100x Stock Solution purchased from Vendor (ATCC Mineral Mix)
NaCl	1.7	100x Stock Solution purchased from Vendor (ATCC Mineral Mix)
NiCl2	0.015	100x Stock Solution purchased from Vendor (ATCC Mineral Mix)
Potassium Hydroxide	4.5E-04	100x Stock Solution purchased from Vendor (ATCC Mineral Mix)
Sodium Sulfate	7.0	100x Stock Solution purchased from Vendor (ATCC Mineral Mix)
ZnSO4	0.062	100x Stock Solution purchased from Vendor (ATCC Mineral Mix)
Ca-D-pantothenate	4.2E-04	100x vitamin mix solution (ANL Vitamin Mix)
Cobalamin (B12)	1.5E-06	100x vitamin mix solution (ANL Vitamin Mix)
Pyridoxine HCl	9.7E-04	100x vitamin mix solution (ANL Vitamin Mix)
Riboflavin	5.3E-04	100x vitamin mix solution (ANL Vitamin Mix)
Tetrahydrofolic Acid	2.8E-06	100x vitamin mix solution (ANL Vitamin Mix)
Thiamine HCl	5.9E-04	100x vitamin mix solution (ANL Vitamin Mix)

p-Aminobenzoic Acid	0.073	250x 4C Stock Solution (contains p-Aminobenzoic Acid and Pyridoxamine)
Pyridoxamine	0.021	250x 4C Stock Solution (contains p-Aminobenzoic Acid and Pyridoxamine)
Ammonium Chloride	9.3	250x RT Stock Solution (contains MgCl2, KH2PO4, NH4Cl, Nicotinamide)
Magnesium Chloride	1.7	250x RT Stock Solution (contains MgCl2, KH2PO4, NH4Cl, Nicotinamide)
Potassium Phosphate	6.6	250x RT Stock Solution (contains MgCl2, KH2PO4, NH4Cl, Nicotinamide)
Nicotinamide	0.034	250x RT Stock Solution (contains MgCl2, KH2PO4, NH4Cl, Nicotinamide)
Haemin	0.015	250x Stock Solution of Haemin, solubilized with NaOH
Cytosine	5.9E-05	30x Stock Solution purchased from Vendor (10x ACGU Mix)
Guanine	6.0E-05	30x Stock Solution purchased from Vendor (10x ACGU Mix)
L-Adenine	6.0E-05	30x Stock Solution purchased from Vendor (10x ACGU Mix)
Uracil	5.9E-05	30x Stock Solution purchased from Vendor (10x ACGU Mix)
Inositol	6.3	45 g/L Stock Solution
Biotin	0.041	50x Individual Stock Solution (Stored 4°C)
L-alanine	5.3	5x defined amino acid solution (tyrosine added separately)
L-arginine	22	5x defined amino acid solution (tyrosine added separately)
L-asparagine	2.6	5x defined amino acid solution (tyrosine added separately)
L-Aspartic acid	0.40	5x defined amino acid solution (tyrosine added separately)
L-Cysteine	8.4	5x defined amino acid solution (tyrosine added separately)
L-Glutamic acid Sodium	0.66	5x defined amino acid solution (tyrosine added separately)
L-glutamine	2.7	5x defined amino acid solution (tyrosine added separately)
L-Glycine	4.7	5x defined amino acid solution (tyrosine added separately)
L-histidine	1.0	5x defined amino acid solution (tyrosine added separately)
L-isoleucine	1.6	5x defined amino acid solution (tyrosine added separately)
L-leucine	3.6	5x defined amino acid solution (tyrosine added separately)
L-lysine	2.4	5x defined amino acid solution (tyrosine added separately)
L-methionine	0.84	5x defined amino acid solution (tyrosine added separately)
L-phenylalanine	4.5	5x defined amino acid solution (tyrosine added separately)
L-proline	5.9	5x defined amino acid solution (tyrosine added separately)
L-serine	6.4	5x defined amino acid solution (tyrosine added separately)

L-threonine	1.9	5x defined amino acid solution (tyrosine added separately)
L-tryptophan	0.73	5x defined amino acid solution (tyrosine added separately)
L-valine	2.8	5x defined amino acid solution (tyrosine added separately)
L-tyrosine	3.2	Powder
MOPS	72	Powder
Sodium Bicarbonate	48	Powder
L-Arabinose	21	Powder
D-Glucose	25	Powder
Sodium Lactate	28	40% Syrup
Maltose	4	Powder

Table A.3. Lysin Gene Sequences

Protein/Chimera	Sequence
EAD1-CBD1 (Enterolysin A)	ATGAAAAACATCCTTCTGTCCATCTTAGGCGTTTTGTCCATTGTGGTATCACTGGCATTTTCGTCTTATAGTGTTAATG CAGCCTCGAACGAATGGTCGTGGCCTCTGGGCAAGCCTTACGCAGGACGTTATGAAGAGGGCCAACAATTTGGCAA CACGGCTTTTAATCGTGGAGGTACGTACTTCCACGATGGGTTCGATTTTGGGAGCGCTATCTACGGCAATGGAAGCG TATATGCTGTTCACGATGGCAAAATTTTGTATGCAGGGTGGGACCCGGTGGGGGGCGGCTCATTGGGAGCGTTCAT CGTCTTACAGGCAGGTAACACGAACGTGATTTACCAGGAGTTTTCGCGCAATGTAGGCGACATTAAAGTTTCTACGG GCCAAACTGTCAAAAAGGGACAGTTAATCGGGAAGTTCACCTCCTCGCATCTTCATTTGGGCATGACAAAGAAAGAA TGGCGCTCGGCCCACAGCTCATGGAACAAGGACGACGGGACTTGGTTCAACCCTATTCCTATCCTTCAGGGTGGAA GCACCCCGACGCCCCCAAATCCTGGCCCGAAGAACTTCACCACAAACGTCCGCTATGGACTTCGTGTCCTTGGTGG CTCATGGCTGCCGGAGGTAACAAATTTTAACAACACTAACGATGGATTTGCTGGTTATCCTAACCGCCAGCACGATAT GCTGTACATCAAAGTTGATAAGGGGCAGATGAAATACCGCGTCCATACCGCACAATCCGGGTGGCTTCCGTGGGTA TCGAAAGGCGACAAATCCGATACAGTTAATGGCGCTGCCGGAATGCCAGGTCAGGCGATCGATGGTGTCCAATTAA ATTACATCACTCCCAAAGGAGAAAAACTGTCCCAAGCGTATTACCGCAGCCAAACCACCAAACGCAGCGGGTGGTTA AAGGTATCTGCTGACAATGGTTCGATTCCTGGTCTGGATTCATACGCAGGCATCTTTGGGGAACCCTTAGATCGCTT ACAAATCGGTATTTCACAGTCAAACCCATTC
EAD1-CBD2	ATGAAAAACATCCTTCTGTCCATCTTAGGCGTTTTGTCCATTGTGGTATCACTGGCATTTTCGTCTTATAGTGTTAATG CAGCCTCGAACGAATGGTCGTGGCCTCTGGGCAAGCCTTACGCAGGACGTTATGAAGAGGGCCAACAATTTGGCAA CACGGCTTTTAATCGTGGAGGTACGTACTTCCACGATGGGTTCGATTTTGGGAGCGCTATCTACGGCAATGGAAGCG TATATGCTGTTCACGATGGCAAAATTTTGTATGCAGGGTGGGACCCGGTGGGGGGCGGCTCATTGGGAGCGTTCAT CGTCTTACAGGCAGGTAACACGAACGTGATTTACCAGGAGTTTTCGCGCAATGTAGGCGACATTAAAGTTTCTACGG GCCAAACTGTCAAAAAGGGACAGTTAATCGGGAAGTTCACCTCCTCGCATCTTCATTTGGGCATGACAAAGAAAGAA TGGCGCTCGGCCCACAGCTCATGGAACAAGGACGACGGGACTTGGTTCAACCCTATTCCTATCCTTCAGGGTGGAA GCACCCCGACGCCCCCAAATCCTGGCCCGAAGAACTTCACTACGGTATCGTATGGCCTTCGTCAGATCGGGGCGGG TTGGCTTGGAACAATCACGGATTTCAATAACTCGAACGGAAACGGCTTCGCCGGCAATAGCAATCACGAACACGATA TGCTTTTTGCTTCTGTGTCCCATGGCTCGCTGCGGTATCGCGTTCACACGGTCAAGAGCGGTTGGTTGGGTTGGGTA AATCAGGGCAATAAAAATGATTTGGTGAATGGTTGCGCTGGCAATCCAAATGAGGCCATAGACGGGGTTCAGTTTTA TTATACAACACCTAACGGGGAAGTGTATAAACAAGCCTACTACCGCAGTCAAACGAGTAAGCGGGCGGGGTGGCTT CCGTCGGTCGAGGATGATAAAGACTTTGCTGGAATACTGGGCGAACCACTTGATAGATTGCAAATTGCCATCCGCTC TTCTAACCCATTCTGA

EAD1-CBD3	ATGAAAAACATCCTTCTGTCCATCTTAGGCGTTTTGTCCATTGTGGTATCACTGGCATTTTCGTCTTATAGTGTTAATG CAGCCTCGAACGAATGGTCGTGGCCTCTGGGCAAGCCTTACGCAGGACGTTATGAAGAGGGCCAACAATTTGGCAA CACGGCTTTTAATCGTGGAGGTACGTACTTCCACGATGGGTTCGATTTTGGGAGCGCTATCTACGGCAATGGAAGCG TATATGCTGTTCACGATGGCAAAATTTTGTATGCAGGGTGGGACCCGGTGGGGGGCGGCTCATTGGGAGCGTTCAT CGTCTTACAGGCAGGTAACACGAACGTGATTTACCAGGAGTTTTCGCGCAATGTAGGCGACATTAAAGTTTCTACGG GCCAAACTGTCAAAAAGGGACAGTTAATCGGGAAGTTCACCTCCTCGCATCTTCATTTGGGCATGACAAAGAAAGAA TGGCGCTCGGCCCACAGCTCATGGAACAAGGACGACGGGACTTGGTTCAACCCTATTCCTATCCTTCAGGGTGGAA GCACCCCGACGCCCCCAAATCCTGGCCCGAAGAACTTCACTACGGTGACTTACGGGTTACATGTAAAAGGCGGTGA TTGGCTGTCCCCAGTAGTTAATTTCAATCCCGTCAATTCGGACGGGTATGCTGGCTTACCTAACCACGAACATGATAT GCTGTATGCGCGGGTCGATCATGGTGCGCTGAAGTATCGGGTACACACTATTGAGGCTGGCTGGCTGGACTGGGTA ACGTCGGGGAATCCAAACGATCCAGTCAACGGGTGTGCTGGCATGTTTGGACAGACTATTGACGGAGTCCAGATGG TCTATCTTACGCCTTCGGGGGAATACTACCGTAATGCGTATTATCGGTCGCAGACCACCAAACGGGCCGATTGGTTA CCGGAGGTAGCCGATGATAGTGATTTCGCGGGAATATTTGGGGAACCCCTGGATCGCTTGCAGGCAGCGGTCAACA TCCGCGATCCCTTTGGGGAACAATGA
EAD2-CBD1	ATGGCGAATGATTGGGGATGGCCTTTTAGCGGAGGCTACAAAGGGTATGAAGAAGGACAACAATTTGGAATGACTAC ATACGATCGGACGGGCAGAGGGGACTATTTTCATGACGGCTTTGACTTTGGCTCAGCGAAATATCCGGGGTCTAACA TCGCAGCCGTGCACGCAGGGACTGTGGTATACGCGGGCTGGGCTCCTGCGGGTTACGGGGCACTGGGCACGGTC GTTGTTACGAAGGATTCAAGCGGCTATTACGTCGTCTACCAGGAATTTGGCACGTCAACATCAAACATAAACGTCTCT GTAGGCCAGTCAGTGACTCTTGGACAAGTAATAGGGACACGCAATACCTCTCACCTGCACCTGGGGATCACTAAGAA AGACTGGCTGTCTGCCCAGTCGTCGGCCTTCAAAGACGACGGGACGTGGCTTAATCCTATCAACATAATACAGAACG GTACTACGCCCACGCCGCCGAATCCAGGACCTAAGAATTTCACTACGAACGTCCGCTATGGACTTCGTGTCCTTGGT GGCTCATGGCTGCCGGAGGTAACAAATTTTAACAACACTAACGATGGATTTGCTGGTTATCCTAACCGCCAGCACGA TATGCTGTACATCAAAGTTGATAAGGGGCAGATGAAATACCGCGTCCATACCGCACAATCCGGGTGGCTTCCGTGG GTATCGAAAGGCGACAAATCCGATACAGTTAATGGCGCTGCCGGAATGCCAGGTCAGGCGATCGATGGTGTCCAAT TAAATTACATCACTCCCAAAGGAGAAAAACTGTCCCAAGCGTATTACCGCAGCCAAACCACCAAACGCAGCGGGTGG TTAAAGGTATCTGCTGACAATGGTTCGATTCCTGGTCTGGATTCATACGCAGGCATCTTTGGGGAACCCTTAGATCG CTTACAAATCGGTATTTCACAGTCAAACCCATTCTGA

EAD2-CBD2	ATGGCGAATGATTGGGGATGGCCTTTTAGCGGAGGCTACAAAGGGTATGAAGAAGGACAACAATTTGGAATGACTAC ATACGATCGGACGGGCAGAGGGGACTATTTTCATGACGGCTTTGACTTTGGCTCAGCGAAATATCCGGGGTCTAACA TCGCAGCCGTGCACGCAGGGACTGTGGTATACGCGGGCTGGGCTCCTGCGGGTTACGGGGCACTGGGCACGGTC GTTGTTACGAAGGATTCAAGCGGCTATTACGTCGTCTACCAGGAATTTGGCACGTCAACATCAAACATAAACGTCTCT GTAGGCCAGTCAGTGACTCTTGGACAAGTAATAGGGACACGCAATACCTCTCACCTGCACCTGGGGATCACTAAGAA AGACTGGCTGTCTGCCCAGTCGTCGGCCTTCAAAGACGACGGGACGTGGCTTAATCCTATCAACATAATACAGAACG GTACTACGCCCACGCCGCCGAATCCAGGACCTAAGAATTTCACTACGGTATCGTATGGCCTTCGTCAGATCGGGGC GGGTTGGCTTGGAACAATCACGGATTTCAATAACTCGAACGGAAACGGCTTCGCCGGCAATAGCAATCACGAACAC GATATGCTTTTTGCTTCTGTGTCCCATGGCTCGCTGCGGTATCGCGTTCACACGGTCAAGAGCGGTTGGTTGGGTTG GGTAAATCAGGGCAATAAAAATGATTTGGTGAATGGTTGCGCTGGCAATCCAAATGAGGCCATAGACGGGGTTCAGT TTTATTATACAACACCTAACGGGGAAGTGTATAAACAAGCCTACTACCGCAGTCAAACGAGTAAGCGGGCGGGGTGG CTTCCGTCGGTCGAGGATGATAAAGACTTTGCTGGAATACTGGGCGAACCACTTGATAGATTGCAAATTGCCATCCG CTCTTCTAACCCATTCTGA
EAD2-CBD3	ATGGCGAATGATTGGGGATGGCCTTTTAGCGGAGGCTACAAAGGGTATGAAGAAGGACAACAATTTGGAATGACTAC ATACGATCGGACGGGCAGAGGGGACTATTTTCATGACGGCTTTGACTTTGGCTCAGCGAAATATCCGGGGTCTAACA TCGCAGCCGTGCACGCAGGGACTGTGGTATACGCGGGCTGGGCTCCTGCGGGTTACGGGGCACTGGGCACGGTC GTTGTTACGAAGGATTCAAGCGGCTATTACGTCGTCTACCAGGAATTTGGCACGTCAACATCAAACATAAACGTCTCT GTAGGCCAGTCAGTGACTCTTGGACAAGTAATAGGGACACGCAATACCTCTCACCTGCACCTGGGGATCACTAAGAA AGACTGGCTGTCTGCCCAGTCGTCGGCCTTCAAAGACGACGGGACGTGGCTTAATCCTATCAACATAATACAGAACG GTACTACGCCCACGCCGCCGAATCCAGGACCTAAGAATTTCACTACGGTGACTTACGGGTTACATGTAAAAGGCGGT GATTGGCTGTCCCCAGTAGTTAATTTCAATCCCGTCAATTCGGACGGGTATGCTGGCTTACCTAACCACGAACATGAT ATGCTGTATGCGCGGGTCGATCATGGTGCGCTGAAGTATCGGGTACACACTATTGAGGCTGGCTGGCTGGACTGGG TAACGTCGGGGAATCCAAACGATCCAGTCAACGGGTGTGCTGGCATGTTTGGACAGACTATTGACGGAGTCCAGAT GGTCTATCTTACGCCTTCGGGGGAATACTACCGTAATGCGTATTATCGGTCGCAGACCACCAAACGGGCCGATTGGT TACCGGAGGTAGCCGATGATAGTGATTTCGCGGGAATATTTGGGGAACCCCTGGATCGCTTGCAGGCAGCGGTCAA CATCCGCGATCCCTTTGGGGAACAATGA

EAD3-CBD1	ATGGGAATATGGCGTCTTCCATTCGATGGTCAGTTAAAACCCTACGAAGAGGGACAGCAGTTCGGTAATACGAAATA TCCTCGGGGGAGAGGCTATTTTCACGATGGATATGATTTCGGTTCGGCAAAATACTCCGGGAATTTCAAGGCGGTTA ACGATGGAAAAGTCATTTTCGCAGGTTATTATGGGGGCGCGGTGGGCTATGCCATTGTTTTACAAATAGCAGAGTAT CAAGTTATGTATCAGAAGTTTGGGTCAACTTTCTTTGTAAAAGCAGGGGACACGGTAAAAGTAGGTCAGGCGCTTGG AACTTTAACTAGCAATCATTTGCACGTCGGAATCACGAAAAAAGACTGGCGCACTGCGCTGAGTTCCTGGGATATAG ATGATGGCACATGGTTGAACCCAATACCGATATTAACAAGCGGTGGAACGCCCACGCCGCCGAATCCAGGACCTAA GAATTTCACTACGAACGTCCGCTATGGACTTCGTGTCCTTGGTGGCTCATGGCTGCCGGAGGTAACAAATTTTAACA ACACTAACGATGGATTTGCTGGTTATCCTAACCGCCAGCACGATATGCTGTACATCAAAGTTGATAAGGGGCAGATG AAATACCGCGTCCATACCGCACAATCCGGGTGGCTTCCGTGGGTATCGAAAGGCGACAAATCCGATACAGTTAATG GCGCTGCCGGAATGCCAGGTCAGGCGATCGATGGTGTCCAATTAAATTACATCACTCCCAAAGGAGAAAAACTGTCC CAAGCGTATTACCGCAGCCAAACCACCAAACGCAGCGGGTGGTTAAAGGTATCTGCTGACAATGGTTCGATTCCTGG TCTGGATTCATACGCAGGCATCTTTGGGGAACCCTTAGATCGCTTACAAATCGGTATTTCACAGTCAAACCCATTCTG A
EAD3-CBD2	ATGGGAATATGGCGTCTTCCATTCGATGGTCAGTTAAAACCCTACGAAGAGGGACAGCAGTTCGGTAATACGAAATA TCCTCGGGGGAGAGGCTATTTTCACGATGGATATGATTTCGGTTCGGCAAAATACTCCGGGAATTTCAAGGCGGTTA ACGATGGAAAAGTCATTTTCGCAGGTTATTATGGGGGCGCGGTGGGCTATGCCATTGTTTTACAAATAGCAGAGTAT CAAGTTATGTATCAGAAGTTTGGGTCAACTTTCTTTGTAAAAGCAGGGGACACGGTAAAAGTAGGTCAGGCGCTTGG AACTTTAACTAGCAATCATTTGCACGTCGGAATCACGAAAAAAGACTGGCGCACTGCGCTGAGTTCCTGGGATATAG ATGATGGCACATGGTTGAACCCAATACCGATATTAACAAGCGGTGGAACGCCCACGCCGCCGAATCCAGGACCTAA GAATTTCACTACGGTATCGTATGGCCTTCGTCAGATCGGGGCGGGTTGGCTTGGAACAATCACGGATTTCAATAACT CGAACGGAAACGGCTTCGCCGGCAATAGCAATCACGAACACGATATGCTTTTTGCTTCTGTGTCCCATGGCTCGCTG CGGTATCGCGTTCACACGGTCAAGAGCGGTTGGTTGGGTTGGGTAAATCAGGGCAATAAAAATGATTTGGTGAATGG TTGCGCTGGCAATCCAAATGAGGCCATAGACGGGGTTCAGTTTTATTATACAACACCTAACGGGGAAGTGTATAAAC AAGCCTACTACCGCAGTCAAACGAGTAAGCGGGCGGGGTGGCTTCCGTCGGTCGAGGATGATAAAGACTTTGCTGG AATACTGGGCGAACCACTTGATAGATTGCAAATTGCCATCCGCTCTTCTAACCCATTCTGA

EAD3-CBD3	ATGGGAATATGGCGTCTTCCATTCGATGGTCAGTTAAAACCCTACGAAGAGGGACAGCAGTTCGGTAATACGAAATA TCCTCGGGGGAGAGGCTATTTTCACGATGGATATGATTTCGGTTCGGCAAAATACTCCGGGAATTTCAAGGCGGTTA ACGATGGAAAAGTCATTTTCGCAGGTTATTATGGGGGCGCGGTGGGCTATGCCATTGTTTTACAAATAGCAGAGTAT CAAGTTATGTATCAGAAGTTTGGGTCAACTTTCTTTGTAAAAGCAGGGGACACGGTAAAAGTAGGTCAGGCGCTTGG AACTTTAACTAGCAATCATTTGCACGTCGGAATCACGAAAAAAGACTGGCGCACTGCGCTGAGTTCCTGGGATATAG ATGATGGCACATGGTTGAACCCAATACCGATATTAACAAGCGGTGGAACGCCCACGCCGCCGAATCCAGGACCTAA GAATTTCACTACGGTGACTTACGGGTTACATGTAAAAGGCGGTGATTGGCTGTCCCCAGTAGTTAATTTCAATCCCGT CAATTCGGACGGGTATGCTGGCTTACCTAACCACGAACATGATATGCTGTATGCGCGGGTCGATCATGGTGCGCTG AAGTATCGGGTACACACTATTGAGGCTGGCTGGCTGGACTGGGTAACGTCGGGGAATCCAAACGATCCAGTCAACG GGTGTGCTGGCATGTTTGGACAGACTATTGACGGAGTCCAGATGGTCTATCTTACGCCTTCGGGGGAATACTACCGT AATGCGTATTATCGGTCGCAGACCACCAAACGGGCCGATTGGTTACCGGAGGTAGCCGATGATAGTGATTTCGCGG GAATATTTGGGGAACCCCTGGATCGCTTGCAGGCAGCGGTCAACATCCGCGATCCCTTTGGGGAACAATGA
EAD1-CBD1-Strep tag	ATGAAAAACATCCTTCTGTCCATCTTAGGCGTTTTGTCCATTGTGGTATCACTGGCATTTTCGTCTTATAGTGTTAATG CAGCCTCGAACGAATGGTCGTGGCCTCTGGGCAAGCCTTACGCAGGACGTTATGAAGAGGGCCAACAATTTGGCAA CACGGCTTTTAATCGTGGAGGTACGTACTTCCACGATGGGTTCGATTTTGGGAGCGCTATCTACGGCAATGGAAGCG TATATGCTGTTCACGATGGCAAAATTTTGTATGCAGGGTGGGACCCGGTGGGGGGCGGCTCATTGGGAGCGTTCAT CGTCTTACAGGCAGGTAACACGAACGTGATTTACCAGGAGTTTTCGCGCAATGTAGGCGACATTAAAGTTTCTACGG GCCAAACTGTCAAAAAGGGACAGTTAATCGGGAAGTTCACCTCCTCGCATCTTCATTTGGGCATGACAAAGAAAGAA TGGCGCTCGGCCCACAGCTCATGGAACAAGGACGACGGGACTTGGTTCAACCCTATTCCTATCCTTCAGGGTGGAA GCACCCCGACGCCCCCAAATCCTGGCCCGAAGAACTTCACCACAAACGTCCGCTATGGACTTCGTGTCCTTGGTGG CTCATGGCTGCCGGAGGTAACAAATTTTAACAACACTAACGATGGATTTGCTGGTTATCCTAACCGCCAGCACGATAT GCTGTACATCAAAGTTGATAAGGGGCAGATGAAATACCGCGTCCATACCGCACAATCCGGGTGGCTTCCGTGGGTA TCGAAAGGCGACAAATCCGATACAGTTAATGGCGCTGCCGGAATGCCAGGTCAGGCGATCGATGGTGTCCAATTAA ATTACATCACTCCCAAAGGAGAAAAACTGTCCCAAGCGTATTACCGCAGCCAAACCACCAAACGCAGCGGGTGGTTA AAGGTATCTGCTGACAATGGTTCGATTCCTGGTCTGGATTCATACGCAGGCATCTTTGGGGAACCCTTAGATCGCTT ACAAATCGGTATTTCACAGTCAAACCCATTCGGGGGGGGGAGCGGTGGAGGCTCCGGCGGTTCAGCTTGGTCACAC CCACAGTTTGAAAAATGA

Strep tag -EAD2-CBD2	ATGTGGAGCCACCCGCAGTTCGAAAAGATGGCGAATGATTGGGGATGGCCTTTTAGCGGAGGCTACAAAGGGTATG AAGAAGGACAACAATTTGGAATGACTACATACGATCGGACGGGCAGAGGGGACTATTTTCATGACGGCTTTGACTTT GGCTCAGCGAAATATCCGGGGTCTAACATCGCAGCCGTGCACGCAGGGACTGTGGTATACGCGGGCTGGGCTCCT GCGGGTTACGGGGCACTGGGCACGGTCGTTGTTACGAAGGATTCAAGCGGCTATTACGTCGTCTACCAGGAATTTG GCACGTCAACATCAAACATAAACGTCTCTGTAGGCCAGTCAGTGACTCTTGGACAAGTAATAGGGACACGCAATACC TCTCACCTGCACCTGGGGATCACTAAGAAAGACTGGCTGTCTGCCCAGTCGTCGGCCTTCAAAGACGACGGGACGT GGCTTAATCCTATCAACATAATACAGAACGGTACTACGCCCACGCCGCCGAATCCAGGACCTAAGAATTTCACTACG GTATCGTATGGCCTTCGTCAGATCGGGGCGGGTTGGCTTGGAACAATCACGGATTTCAATAACTCGAACGGAAACG GCTTCGCCGGCAATAGCAATCACGAACACGATATGCTTTTTGCTTCTGTGTCCCATGGCTCGCTGCGGTATCGCGTT CACACGGTCAAGAGCGGTTGGTTGGGTTGGGTAAATCAGGGCAATAAAAATGATTTGGTGAATGGTTGCGCTGGCA ATCCAAATGAGGCCATAGACGGGGTTCAGTTTTATTATACAACACCTAACGGGGAAGTGTATAAACAAGCCTACTACC GCAGTCAAACGAGTAAGCGGGCGGGGTGGCTTCCGTCGGTCGAGGATGATAAAGACTTTGCTGGAATACTGGGCG AACCACTTGATAGATTGCAAATTGCCATCCGCTCTTCTAACCCATTCTGA